

1 **A global hotspot for dissolved organic carbon in hypermaritime watersheds of coastal**  
2 **British Columbia.**

3  
4 Allison A. Oliver<sup>1,2</sup>, Suzanne E. Tank<sup>1,2</sup>, Ian Giesbrecht<sup>2,7</sup>, Maartje C. Korver<sup>2</sup>, William C.  
5 Floyd<sup>3,4,2</sup>, Paul Sanborn<sup>5,2</sup>, Chuck Bulmer<sup>6</sup>, Ken P. Lertzman<sup>7,2</sup>

6  
7 <sup>1</sup>University of Alberta, Department of Biological Sciences, CW 405, Biological Sciences Bldg.,  
8 University of Alberta, Edmonton, Alberta, T6G 2E9, Canada

9 <sup>2</sup>Hakai Institute, Tula Foundation, Box 309, Heriot Bay, British Columbia, V0P 1H0, Canada

10 <sup>3</sup>Ministry of Forests, Lands and Natural Resource Operations, 2100 Labieux Rd, Nanaimo, BC,  
11 V9T 6E9, Canada

12 <sup>4</sup>Vancouver Island University, 900 Fifth Street, Nanaimo, BC, V9R 5S5, Canada

13 <sup>5</sup>Ecosystem Science and Management Program, University of Northern British Columbia, 3333  
14 University Way, Prince George, BC, V2N 4Z9, Canada

15 <sup>6</sup>BC Ministry of Forests Lands and Natural Resource Operations, 3401 Reservoir Rd, Vernon,  
16 BC, V1B 2C7, Canada

17 <sup>7</sup>School of Resource and Environmental Management, Simon Fraser University, TASC 1- Room  
18 8405, 8888 University Drive, Burnaby, BC, V5A 1S6, Canada

19  
20  
21 Corresponding author: [aaoliver@ualberta.ca](mailto:aaoliver@ualberta.ca)

34 **Abstract**

35           The perhumid region of the coastal temperate rainforest (CTR) of Pacific North America  
36 is one of the wettest places on Earth and contains numerous small catchments that discharge  
37 freshwater and high concentrations of dissolved organic carbon (DOC) directly to the coastal  
38 ocean. However, empirical data on the flux and composition of DOC exported from these  
39 watersheds is scarce. We established monitoring stations at the outlets of seven catchments on  
40 Calvert and Hecate Islands, British Columbia, which represent the rain dominated hypermaritime  
41 region of the perhumid CTR. Over several years, we measured stream discharge, stream water  
42 DOC concentration, and stream water dissolved organic matter (DOM) composition. Discharge  
43 and DOC concentrations were used to calculate DOC fluxes and yields, and DOM composition  
44 was characterized using absorbance and fluorescence spectroscopy with parallel factor analysis  
45 (PARAFAC). The areal estimate of annual DOC yield in water year 2015 was 33.3 Mg C km<sup>-2</sup>  
46 yr<sup>-1</sup>, with individual watersheds ranging from an average of 24.1-37.7 Mg C km<sup>-2</sup> yr<sup>-1</sup>. This  
47 represents some of the highest DOC yields to be measured at the coastal margin. We observed  
48 seasonality in the quantity and composition of exports, with the majority of DOC export  
49 occurring during the extended wet period (September-April). Stream flow from catchments  
50 reacted quickly to rain inputs, resulting in rapid export of relatively fresh, highly terrestrial-like  
51 DOM. DOC concentration and measures of DOM composition were related to stream discharge  
52 and stream temperature, and correlated with watershed attributes, including the extent of lakes  
53 and wetlands, and thickness of organic and mineral soil horizons. Our discovery of high DOC  
54 yields from these small catchments in the CTR is especially compelling as they deliver relatively  
55 fresh, highly terrestrial organic matter directly to the coastal ocean. Hypermaritime landscapes  
56 are common on the British Columbia coast, suggesting that this coastal margin may play an

57 important role in the global processing of carbon and in linking terrestrial carbon to marine  
58 ecosystems.

## 59 **1. Introduction**

60 Freshwater aquatic ecosystems process and transport a significant amount of carbon  
61 (Cole et al., 2007; Aufdenkampe et al., 2011; Dai et al., 2012). Globally, riverine export is  
62 estimated to deliver around 0.9 Pg C yr<sup>-1</sup> from land to the coastal ocean (Cole et al., 2007), with  
63 typically >50% quantified as dissolved organic carbon (DOC)(Meybeck, 1982; Ludwig et al.,  
64 1996; Alvarez-Cobelas et al., 2012; Mayorga et al., 2010). Rivers draining coastal watersheds  
65 serve as conduits of DOC from terrestrial and freshwater sources to marine environments  
66 (Mulholland and Watts, 1982; Bauer et al., 2013; McClelland et al., 2014) and can have  
67 important implications for coastal carbon cycling, biogeochemical interactions, ecosystem  
68 productivity, and food webs (Hopkinson et al., 1998; Tallis, 2009; Tank et al., 2012; Regnier et  
69 al., 2013). In addition, because the transfer of water and organic matter from watersheds to the  
70 coastal ocean represents an important pathway for carbon cycling and ecological subsidies  
71 between ecosystems, better understanding of these linkages is needed for constraining  
72 predictions of ecosystem productivity in response to perturbations such as climate change. In  
73 regions where empirical data are currently scarce, quantifying land-to-ocean DOC export is  
74 therefore a priority for improving the accuracy of watershed and coastal carbon models (Bauer et  
75 al., 2013).

76 While quantifying DOC flux within and across systems is required for understanding the  
77 magnitude of carbon exchange, the composition of DOC (as dissolved organic matter, or DOM)  
78 is also important for determining the ecological significance of carbon exported from coastal  
79 watersheds. The aquatic DOM pool is a complex mixture that reflects both source material and

80 processing along the watershed terrestrial-aquatic continuum, and as a result can show  
81 significant spatial and temporal variation (Hudson et al., 2007; Graeber et al., 2012; Wallin et al.,  
82 2015). Both DOC concentration and DOM composition can serve as indicators of watershed  
83 characteristics (Koehler et al., 2009), hydrologic flow paths (Johnson et al., 2011; Helton et al.,  
84 2015), and watershed biogeochemical processes (Emili and Price, 2013). DOM composition can  
85 also influence its role in downstream processing and ecological function, such as susceptibility to  
86 biological (Judd et al., 2006) and physiochemical interactions (Yamashita and Jaffé, 2008).

87         The coastal temperate rainforests (CTR) of Pacific North America extend from the Gulf  
88 of Alaska, through British Columbia, to Northern California and span a wide range of  
89 precipitation and climate regimes. Within this rainforest region, the “perhumid” zone has cool  
90 summers and summer precipitation is common (>10% of annual precipitation) (Alaback,  
91 1996)(Fig. 1). The perhumid CTR extends from southeast Alaska through the outer coast of  
92 central British Columbia and contains forests and soils that have accumulated large amounts of  
93 organic carbon above and below ground (Leighty et al., 2006; Gorham et al., 2012). Due to high  
94 amounts of precipitation and close proximity to the coast, this area represents a potential hotspot  
95 for the transport and metabolism of carbon across the land-to-ocean continuum, and quantifying  
96 these fluxes is pertinent for understanding global carbon cycling.

97         Within the large perhumid CTR, there is substantial spatial variation in climate and  
98 landscape characteristics that create uncertainty about carbon cycling and pattern. In Alaska, for  
99 example, riverine DOC concentrations vary with wetland cover (D’Amore et al. 2015a) and  
100 glacial cover (Fellman et al. 2014). Previous studies have shown that streams in southeast Alaska  
101 can contain high DOC concentrations (Fellman et al., 2009a; D’Amore et al., 2015a) and  
102 produce high DOC yields (D’Amore et al., 2015b; D’Amore et al., 2016, Stackpoole et al.,



103 2016), but no known field estimates have been generated for the perhumid CTR of British  
104 Columbia, an area of approximately 97,824 km<sup>2</sup> (adapted from Wolf et al., 1995). Within the  
105 perhumid CTR of British Columbia, terrestrial ecologists have defined a large (29,935 km<sup>2</sup>)  
106 *hypermaritime* sub-region where rainfall dominates over snow, seasonality is moderated by the  
107 ocean, and wetlands are extensive (Pojar et al., 1991; area estimated using British Columbia  
108 Biogeoclimatic Ecosystem Classification Subzone/Variant mapping Version 10, August 31,  
109 2016, available at: [https://catalogue.data.gov.bc.ca/dataset/f358a53b-ffde-4830-a325-](https://catalogue.data.gov.bc.ca/dataset/f358a53b-ffde-4830-a325-a5a03ff672c3)  
110 [a5a03ff672c3](https://catalogue.data.gov.bc.ca/dataset/f358a53b-ffde-4830-a325-a5a03ff672c3)). Previous work in the hypermaritime CTR showed that DOC concentrations are  
111 high in small streams and tend to increase during rain events (Gibson et al., 2000; Fitzgerald et  
112 al., 2003; Emili and Price, 2013). Taken together, these conditions should be expected to  
113 generate high yields and fluxes of DOC from hypermaritime watersheds to the coastal ocean.

114 The objectives of this study were to provide the first field-based estimates of DOC  
115 exports from watersheds in the extensive hypermaritime region of British Columbia's perhumid  
116 CTR, to describe the temporal and spatial dynamics of exported DOC concentration and DOM  
117 composition, and to identify relationships between DOC concentration, DOM composition, and  
118 watershed characteristics.

## 119 **2. Methods**

### 120 **2.1 Study Sites**

121 Study sites are located on northern Calvert Island and adjacent Hecate Island on the  
122 central coast of British Columbia, Canada (Lat 51.650, Long -128.035; Fig. 1). Average annual  
123 precipitation and air temperature at sea level from 1981-2010 was 3356 mm yr<sup>-1</sup> and 8.4 °C  
124 (average annual min= 0.9°C, average annual max= 17.9°C) (available online at  
125 <http://www.climatewna.com/>; Wang et al., 2012), with precipitation dominated by rain, and

126 winter snowpack persisting only at higher elevations. Sites are located within the hypermaritime  
127 region of the CTR on the outer coast of British Columbia. Soils overlying the granodiorite  
128 bedrock (Roddick, 1996) are usually < 1 m thick, and have formed in sandy colluvium and  
129 patchy morainal deposits, with limited areas of coarse glacial outwash. Chemical weathering and  
130 organic matter accumulation in the cool, moist climate have produced soils dominated by  
131 Podzols and Follic Histosols, with Hemists up to 2 m thick in depressional sites (IUSS Working  
132 Group WRB, 2015). The landscape is comprised of a mosaic of ecosystem types, including  
133 exposed bedrock, extensive wetlands, bog forests and woodlands, with organic rich soils (Green,  
134 2014; Thompson et al., 2016). Forest stands are generally short with open canopies reflecting the  
135 lower productivity of the hypermaritime forests compared to the rest of the perhumid CTR  
136 (Banner et al., 2005). Dominant trees are western redcedar, yellow-cedar, shore pine and western  
137 hemlock with composition varying across topographic and edaphic gradients. Widespread  
138 understory plants include bryophytes, salal, deer fern, and tufted clubrush. Wetland plants are  
139 locally abundant including diverse *Sphagnum* mosses and sedges. Although the watersheds have  
140 no history of mining or industrial logging, archaeological evidence suggests that humans have  
141 occupied this landscape for at least 13,000 years (McLaren et al., 2014). This occupation has had  
142 a local effect on forest productivity near habitation sites (Trant et al., 2016) and on fire regimes  
143 (Hoffman et al., 2016). We selected seven watersheds with streams draining directly into the  
144 ocean (Fig. 1). These numbered watersheds (626, 693, 703, 708, 819 844, and 1015) range in  
145 size (3.2 to 12.8 km<sup>2</sup>) and topography (maximum elevation 160 m to 1012 m), are variably  
146 affected by lakes (0.3 – 9.1% lake coverage), and – as is characteristic of the perhumid CTR–  
147 have a high degree of wetland coverage (24– 50%) (Table 1).

## 148 **2.2 Soils and watershed characteristics**

149 Watersheds and streams were delineated using a 3 m resolution digital elevation model  
150 (DEM) derived from airborne laser scanning (LiDAR) and flow accumulation analysis using  
151 geographic information systems (GIS) to summarize watershed characteristics for each  
152 watershed polygon and for all watersheds combined (Gonzalez Arriola et al., 2015; Table 1).  
153 Topographic measures were estimated from the DEM, and lake and wetland cover estimated  
154 from Province of British Columbia Terrestrial Ecosystem Mapping (TEM) (Green, 2014), and  
155 soil material thickness estimated from unpublished digital soil maps (Supplemental S1). We  
156 recorded thickness of organic soil material, thickness of mineral soil material, and total soil depth  
157 to bedrock at a total of 353 field sites. Mineral soil horizons have  $\leq 17\%$  organic C, while  
158 organic soil horizons have  $> 17\%$  organic C, per the Canadian System of Soil Classification (Soil  
159 Classification Working Group, 1998). In addition to field-sampled sites, 40 sites with exposed  
160 bedrock (0 cm soil depth) were located using aerial photography. Soil thicknesses were  
161 combined with a suite of topographic, vegetation, and remote sensing (LiDAR and RapidEye  
162 satellite imagery) data for each sampling point and used to train a random forest model  
163 (randomForest package in R; Liaw and Wiener, 2002) that was used to predict soil depth values.  
164 Soil material thicknesses were then averaged for each watershed (Table 1). For additional details  
165 on field site selection and methods used for predictions of soil thickness, see Supplemental S1.1.

### 166 **2.3 Sample Collection and Analysis**

167 From May 2013 to July 2016, we collected stream water grab samples from each  
168 watershed stream outlet every 2-3 weeks ( $n_{\text{total}} = 402$ ), with less frequent sampling ( $\sim$  monthly)  
169 during winter (Fig. 1). All samples were filtered in the field (Millipore Millex-HP Hydrophilic  
170 PES 0.45 $\mu\text{m}$ ) and kept in the dark, on ice until analysis. DOC samples were filtered into 60 mL  
171 amber glass bottles and preserved with 7.5M  $\text{H}_3\text{PO}_4$ . Fe samples were filtered into 125 mL

172 HDPE bottles and preserved with 8M HNO<sub>3</sub>. DOC and Fe samples were analyzed at the BC  
173 Ministry of the Environment Technical Services Laboratory (Victoria, BC, Canada). DOC  
174 concentrations were determined on a TOC analyzer (Aurora 1030; OI-Analytical) using wet  
175 chemical oxidation with persulfate followed by infrared detection of CO<sub>2</sub>. Fe concentrations  
176 were determined on a dual-view ICP-OES spectrophotometer (Prodigy; Teledyne Leeman Labs)  
177 using a Seaspray pneumatic nebulizer.

178 In May 2014, we began collecting stream samples for stable isotopic composition of  $\delta^{13}\text{C}$   
179 in DOC ( $\delta^{13}\text{C}$ -DOC; n= 173) and optical characterization of DOM using absorbance  
180 spectroscopy (n= 259). Beginning in January 2016, we also analyzed samples using fluorescence  
181 spectroscopy (see section 2.6). Samples collected for  $\delta^{13}\text{C}$ -DOC were filtered into 40 mL EPA  
182 glass vials and preserved with H<sub>3</sub>PO<sub>4</sub>.  $\delta^{13}\text{C}$ -DOC samples were analyzed at GG Hatch Stable  
183 Isotope Laboratory (Ottawa, ON, Canada) using high temperature combustion (TIC-TOC  
184 Combustion Analyser Model 1030; OI Analytical) coupled to a continuous flow isotope ratio  
185 mass spectrometry (Finnigan Mat DeltaPlusXP; Thermo Fischer Scientific)(Lalonde et al. 2014).  
186 Samples analyzed for optical characterization using absorbance and fluorescence were filtered  
187 into 125 mL amber HDPE bottles and analyzed at the Hakai Institute (Calvert Island, BC,  
188 Canada) within 24 hours of collection.

#### 189 **2.4 Hydrology: Precipitation and Stream Discharge**

190 We measured precipitation using a TB4-L tipping bucket rain gauge with a 0.2 mm  
191 resolution (Campbell Scientific Ltd.) located in watershed 708 (elevation= 16 m a.s.l). The rain  
192 gauge was calibrated twice per year using a Field Calibration Device, model 653 (HYQUEST  
193 Solutions Ltd).

194 We determined continuous stream discharge for each watershed by developing stage  
195 discharge rating curves at fixed hydrometric stations situated in close proximity to each stream  
196 outlet. Sites were located above tidewater influence and were selected based on favourable  
197 conditions (i.e., channel stability and stable hydraulic conditions) for the installation and  
198 operation of pressure transducers to measure stream stage. From August 2014 to May 2016 (21  
199 months), we measured stage every 5 minutes using an OTT PLS –L (OTT Hydromet, Colorado,  
200 USA) pressure transducer (0-4 m range SDI-12) connected to a CR1000 (Campbell Scientific,  
201 Edmonton, Canada) data logger. Stream discharge was measured over various intervals using  
202 either the velocity area method (for flows  $< 0.5 \text{ m}^3\text{s}^{-1}$ ; ISO Standard 9196:1992, ISO Standard  
203 748:2007) or salt dilution (for flows  $> 0.5 \text{ m}^3\text{s}^{-1}$ ; Moore, 2005). Rating curves were developed  
204 using the relationship between stream stage height and stream discharge (Supplemental S2).

## 205 **2.5 DOC flux**

206 From October 1, 2014 to April 30, 2016, we estimated DOC flux for each watershed  
207 using measured DOC concentrations (n= 224) and continuous discharge recorded at 15-minute  
208 intervals. The watersheds in this region respond rapidly to rain inputs and as a result DOC  
209 concentrations are highly variable. To address this variability, routine DOC concentration data  
210 (as described in section 2.2) were supplemented with additional grab samples (n= 21) collected  
211 around the peak of the hydrograph during several high flow events throughout the year. We  
212 performed watershed-specific estimates of DOC flux using the “rloadest” package (Lorenz et al.,  
213 2015) in R (version 3.2.5, R Core Team, 2016), which replicates functions developed in the U.S.  
214 Geological Survey load-estimator program, LOADEST (Runkel et al., 2004). LOADEST is a  
215 multiple-regression adjusted maximum likelihood estimation model that calibrates a regression  
216 between measured constituent values and stream flow across seasons and time and then fits it to

217 combinations of coefficients representing nine predetermined models of constituent flux. To  
218 account for potentially small sample size, the best model was selected using the second order  
219 Akaike Information Criterion (AICc) (Akaike, 1981; Hurvich and Tsai, 1989). Input data were  
220 log-transformed to avoid bias and centered to reduce multicollinearity. For additional details on  
221 model selection, see Supplemental Table S3.1.

## 222 **2.6 Optical characterization of DOM**

223 Prior to May 2014, absorbance measures of water samples (n= 99) were conducted on a  
224 Varian Cary-50 (Varian, Inc.) spectrophotometer at the BC Ministry of the Environment  
225 Technical Services Laboratory (Victoria, BC, Canada) to determine specific UV absorption at  
226 254 nm (SUVA<sub>254</sub>). After May 2014, we conducted optical characterization of DOM by  
227 absorbance and fluorescence spectroscopy at the Hakai Institute field station (Calvert Island, BC,  
228 Canada) using an Aqualog fluorometer (Horiba Scientific, Edison, New Jersey, USA). Strongly  
229 absorbing samples (absorbance units > 0.2 at 250 nm) were diluted prior to analysis to avoid  
230 excessive inner filter effects (Lakowicz, 1999). Samples were run in 1 cm quartz cells and  
231 scanned from 220-800 nm at 2 nm intervals to determine SUVA<sub>254</sub> as well as the spectral slope  
232 ratio ( $S_R$ ). SUVA<sub>254</sub> has been shown to positively correlate with increasing molecular aromaticity  
233 associated with the fulvic acid fraction of DOM (Weishaar et al., 2003), and is calculated by  
234 dividing the Decadic absorption coefficient at 254 nm by DOC concentration (mg C L<sup>-1</sup>). To  
235 account for potential Fe interference with absorbance values, we corrected SUVA<sub>254</sub> values by Fe  
236 concentration according the method described in Poulin et al., (2014).  $S_R$  has been shown to  
237 negatively correlate with molecular weight (Helms et al., 2008), and is calculated as the ratio of  
238 the spectral slope from 275 nm to 295 nm ( $S_{275-295}$ ) to the spectral slope from 350 nm to 400 nm  
239 ( $S_{350-400}$ ).

240 We measured excitation and emission spectra (as excitation emission matrices, EEMs) on  
241 samples every three weeks from January to July 2016 (n= 63). Samples were run in 1 cm quartz  
242 cells and scanned from excitation wavelengths of 230-550 nm at 5nm increments, and emission  
243 wavelengths of 210-620 nm at 2 nm increments. The Horiba Aqualog applied the appropriate  
244 instrument corrections for excitation and emission, inner filter effects, and Raman signal  
245 calibration. We calculated the Fluorescence Index and Freshness Index for each EEM. The  
246 Fluorescence Index is often used to indicate DOM source, where higher values are more  
247 indicative of microbial-derived sources of DOM and lower values indicate more terrestrial-  
248 derived sources (McKnight et al., 2001), and is calculated as the ratio of emission intensity at  
249 450 nm to 500 nm, at an excitation of 370 nm. The Freshness Index is used to indicate the  
250 contribution of autochthonous or recently microbial-produced DOM, with higher values  
251 suggesting greater autochthony (i.e., microbial inputs), and is calculated as the ratio of emission  
252 intensity at 380 nm to the maximum emission intensity between 420 nm and 435 nm, at  
253 excitation 310 nm (Wilson and Xenopoulos, 2009).

254 To further characterize features of DOM composition, we performed parallel factor  
255 analysis (PARAFAC) using EEM data within the drEEM toolbox for Matlab (Mathworks, MA,  
256 USA) (Murphy et al., 2013). PARAFAC is a statistical technique used to decompose the  
257 complex mixture of the fluorescing DOM pool into quantifiable, individual components  
258 (Stedmon et al., 2003). We detected a total of six unique components, and validated the model  
259 using core consistency and split-half analysis (Murphy et al., 2013; Stedmon and Bro, 2008).  
260 Components with similar spectra from previous studies were identified using the online  
261 fluorescence repository, OpenFluor (Murphy et al., 2014), and additional components with  
262 similar peaks were identified through literature review. Since the actual chemical structure of

263 fluorophores is unknown, we used the concentration of each fluorophore as maximum  
264 fluorescence of excitation and emission in Raman Units ( $F_{\max}$ ) to derive the percent contribution  
265 of each fluorophore component to total fluorescence. Relationships between PARAFAC  
266 components were also evaluated using Pearson correlation coefficients in the R package “Hmisc”  
267 (Harrell et al., 2016).

## 268 **2.7 Evaluating relationships in DOC concentration and DOM composition with stream** 269 **discharge and temperature**

270 We used linear mixed effects models to assess the relationship between DOC  
271 concentration or DOM composition ( $\delta^{13}\text{C}$ -DOC,  $S_R$ , SUVA<sub>254</sub>, Fluorescence Index, Freshness  
272 Index, PARAFAC components), stream discharge, and stream temperature. Analysis was  
273 performed in R using the nlme package (Pinheiro et al., 2016). Watershed was included as a  
274 random intercept to account for repeat measures on each watershed. For some parameters, a  
275 random slope of either discharge or temperature was also included based on data assessment and  
276 model selection. Model selection was performed using AIC to compare models fit using  
277 Maximum Likelihood (ML) (Burnham and Anderson, 2002; Symonds and Moussalli, 2010). The  
278 final model was fit using Restricted Maximum Likelihood (REML). Marginal  $R^2$ , which  
279 represents an approximation of the proportion of the variance explained by the fixed factors  
280 alone, and conditional  $R^2$ , which represents an approximation of the proportion of the variance  
281 explained by both the fixed and random factors, were calculated based on the methods described  
282 in Nakagawa and Schielzeth (2013) and Johnson (2014).

## 283 **2.8 Redundancy analysis: Relationships between DOC concentration, DOM composition,** 284 **and watershed characteristics**



285 We evaluated relationships between stream water DOC and watershed characteristics by  
286 relating DOC concentration and measures of DOM composition to catchment attributes using  
287 redundancy analysis (RDA; type 2 scaling) in the package `rdaTest` (Legendre and Durand, 2014)  
288 in R (version 3.2.2, R Core Team, 2015). To maximize the amount of information available, we  
289 performed RDA analysis on samples collected from January to July 2016, and therefore included  
290 all parameters of optical characterization (i.e., all PARAFAC components and spectral indices).  
291 We assessed the collinearity of DOM compositional variables using a variance inflation factor  
292 (VIF) criteria of  $> 10$ , which resulted in the removal of PARAFAC components C2, C3, and C5  
293 prior to RDA analysis. Catchment attributes for each watershed included average slope, percent  
294 area of lakes, percent area of wetlands, average depth of mineral soil, and average depth of  
295 organic soil. Relationships between variables were linear, so no transformations were necessary  
296 and variables were standardized prior to analysis. To account for repeat monthly measures per  
297 watershed and potential temporal correlation associated with monthly sampling, we included  
298 sample month as a covariable (“partial-RDA”). To test whether the RDA axes significantly  
299 explained variation in the dataset, we compared permutations of residuals using ANOVA (9,999  
300 iterations; `test.axes` function of `rdaTest`).

### 301 **3. Results**

#### 302 **3.1 Hydrology**

303 We present work for water year 2015 (WY2015; October 1, 2014 – September 30, 2015)  
304 and water year 2016 (WY2016; October 1, 2015 – September, 30, 2016). Annual precipitation  
305 for both water years was lower than historical mean annual precipitation (WY2015= 2661 mm;  
306 WY2016= 2587 mm). It is worth noting that mean annual precipitation at our rain gauge location  
307 ( $2890 \text{ mm yr}^{-1}$ , elevation = 16 m) is substantially lower than the average amount received at

308 higher elevations, which from 1981-2010 was approximately 5027 mm yr<sup>-1</sup> at an elevation of  
309 1000m within our study area. This area receives a very high amount of annual rainfall  
310 (<http://data.worldbank.org>) but also experiences strong seasonal variation, with an extended wet  
311 period from fall through spring, and a much shorter, typically drier period during summer. In  
312 WY2015 and WY2016, 86-88% of the annual precipitation on Calvert Island occurred during the  
313 8-months of wetter and cooler weather between September and April (~ 75% of the year),  
314 designated the “wet period” (WY2015 wet= 2388 mm, average air temp= 7.97°C; WY2016 wet=  
315 2235 mm; average air temp= 7.38°C). The remaining annual precipitation occurred during the  
316 drier and warmer summer months of May – August, designated the “dry period” (WY2015 dry=  
317 314 mm, average air temp= 13.4°C; WY2016 dry= 352 mm, average air temp= 13.1°C). Overall,  
318 although WY2015 was slightly wetter than WY2016, the two years were comparable in relative  
319 precipitation during the wet versus dry periods.

320 Stream discharge (Q) responded rapidly to rain events and as a result, closely tracked  
321 patterns in total precipitation (Fig. 2). Total Q for all watersheds was on average 22% greater for  
322 the wet period of WY2015 (total Q= 223.02 \* 10<sup>6</sup>; range= 5.13 \* 10<sup>6</sup> – 111.51 \* 10<sup>6</sup> m<sup>3</sup>)  
323 compared to the wet period of WY2016 (total Q= 182.89 \* 10<sup>6</sup>; range= 4.17 \* 10<sup>6</sup> – 91.45 \* 10<sup>6</sup>  
324 m<sup>3</sup>). Stream discharge and stream temperature were significantly different for wet versus dry  
325 periods (Mann-Whitney tests, p< 0.0001).

### 326 **3.2 Temporal and spatial patterns in DOC concentration, yield and flux**

327 Stream waters were high in DOC concentration relative to the global average for DOC  
328 concentration in freshwater discharged directly to the ocean (average DOC for Calvert and  
329 Hecate Islands = 10.4 mg L<sup>-1</sup>, std= 3.8; average global DOC= ~ 6 mg L<sup>-1</sup>) (Meybeck, 1982;  
330 Harrison et al., 2005) (Table 1; Fig. 3). Q-weighted average DOC concentrations were higher

331 than average measured DOC concentrations ( $11.1 \text{ mg L}^{-1}$ , Table 1), and also resulted in slightly  
332 different ranking of the watersheds for highest to lowest DOC concentration. Within watersheds,  
333 flow-weighted DOC concentrations ranged from a low of  $8.4 \text{ mg L}^{-1}$  (watershed 693) to a high of  
334  $19.3 \text{ mg L}^{-1}$  (watershed 819), and concentrations were significantly different between watersheds  
335 (Kruskal-Wallis test,  $p < 0.0001$ ). Seasonal variability tended to be higher in watersheds where  
336 DOC concentration was also high (watersheds 626, 819, and 844) and lower in watersheds with  
337 greater lake area (watersheds 1015 and 708) (Table 1; box plots, Figure 3). On an annual basis,  
338 DOC concentrations generally decreased through the wet period, and increased through the dry  
339 period, and concentrations were significantly lower during the wet period compared to the dry  
340 period (Mann-Whitney test,  $p = 0.0123$ ). Results of our linear mixed effects (LME) model  
341 (Supplemental Table S6.1) indicate that DOC concentration was positively related to both  
342 discharge ( $b = 0.613$ ,  $p < 0.001$ ) and temperature ( $b = 0.162$ ,  $p = 0.011$ ) (model conditional  $R^2 =$   
343  $0.57$ , marginal  $R^2 = 0.09$ ).

344 Annual and monthly DOC yields are presented in Table 1. For the total period of  
345 available Q (October 1, 2014 - April 30, 2016; 19 months), areal (all watersheds) DOC yield was  
346  $52.3 \text{ Mg C km}^{-2}$  (95% CI= 45.7 to  $68.2 \text{ Mg C km}^{-2}$ ) and individual watershed yields ranged from  
347  $24.1$  to  $43.6 \text{ Mg C km}^{-2}$ . For WY2015, areal annual DOC yield was  $33.3 \text{ Mg C km}^{-2} \text{ yr}^{-1}$  (95%  
348 CI= 28.9 to  $38.1 \text{ Mg C km}^{-2} \text{ yr}^{-1}$ ). Total monthly rainfall was strongly correlated with monthly  
349 DOC yield (Fig. 4), and average monthly yield for the wet period ( $3.35 \text{ Mg C km}^{-2} \text{ mo}^{-1}$ ; 95%  
350 CI= 2.94 to  $4.40 \text{ Mg C km}^{-2} \text{ mo}^{-1}$ ) was significantly greater than average monthly yield during  
351 the dry period ( $0.50 \text{ Mg C km}^{-2} \text{ mo}^{-1}$ ; 95% CI= 0.41 to  $0.62 \text{ Mg C km}^{-2} \text{ mo}^{-1}$ ) (Mann-Whitney  
352 test,  $p < 0.0001$ ).

353 Across our study watersheds, DOC flux generally increased with increasing watershed  
354 area (Fig. 5). In WY2015, total DOC flux for all watersheds included in our study was 1562 Mg  
355 C (95% CI= 1355 to 1787 Mg C), and individual watershed flux ranged from 82 to  
356 276 Mg C. DOC flux was significantly different in wet versus dry periods (Mann-Whitney test,  $p$   
357  $< 0.0001$ ). Overall, 94% of the export in WY2015 occurred during the wet period, and export for  
358 the wet period of WY2015 was lower than export for the wet period of WY2016 (Fig. 5).

### 359 **3.3 Temporal and spatial patterns in DOM composition**

360 The stable isotopic composition of dissolved organic carbon ( $\delta^{13}\text{C-DOC}$ ) was relatively  
361 tightly constrained over space and time (average  $\delta^{13}\text{C-DOC} = -26.53\text{‰}$ ,  $\text{std} = 0.36$ ; range = -  
362  $27.67\text{‰}$  to  $-24.89\text{‰}$ ). Values of  $S_R$  were low compared to the range typically observed in surface  
363 waters (average  $S_R = 0.78$ ,  $\text{std} = 0.04$ ; range = 0.71 to 0.89) and Fe-corrected  $\text{SUVA}_{254}$  values  
364 were at the high end of the range compared to most surface waters (average  $\text{SUVA}_{254}$  for Calvert  
365 and Hecate Islands =  $4.42 \text{ L mg}^{-1} \text{ m}^{-1}$ ,  $\text{std} = 0.46$ ; range of  $\text{SUVA}_{254}$  in surface waters = 1.0 to 5.0  
366  $\text{L mg}^{-1} \text{ m}^{-1}$ ) (Spencer et al., 2012). Values for both Fluorescence Index (average Fluorescence  
367 Index = 1.36,  $\text{std} = 0.04$ ; range = 1.30 to 1.44) and Freshness Index (average Freshness Index =  
368 0.46,  $\text{std} = 0.02$ ; range = 0.41 to 0.49) were relatively low compared to the typical range found in  
369 surface waters (Fellman et al., 2010; Hansen et al., 2016). Differences between watersheds were  
370 observed for  $\delta^{13}\text{C-DOC}$  (Kruskal-Wallis test,  $p = 0.0043$ ),  $S_R$  (Kruskal-Wallis test,  $p = 0.0001$ ),  
371 Fluorescence Index (Kruskal-Wallis test,  $p = 0.0030$ ), and Freshness Index (Kruskal-Wallis test,  
372  $p = 0.0099$ ), but watersheds did not differ in  $\text{SUVA}_{254}$  (Kruskal-Wallis test,  $p = 0.4837$ ).

373 We did not observe an obvious seasonal trend in  $\delta^{13}\text{C-DOC}$  (Fig. 3), but LME model  
374 results (Supplemental Table S6.1) indicate that  $\delta^{13}\text{C-DOC}$  declined with increasing discharge  
375 ( $b = -0.049$ ,  $p = 0.014$ ) and stream temperature ( $b = -0.024$ ,  $p < 0.001$ ) (model conditional  $R^2 =$

376 0.35, marginal  $R^2 = 0.10$ ). In contrast, although  $SUVA_{254}$  appeared to exhibit a general seasonal  
377 trend of values increasing over the wet period and decreasing over the dry period,  $SUVA_{254}$  was  
378 not significantly related to either discharge or stream temperature in the LME model results.  $S_R$   
379 also appeared to fluctuate seasonally, with lower values during the wet season and higher values  
380 during the dry season.  $S_R$  was negatively related to discharge ( $b = -0.026$ ,  $p < 0.001$ ) and  
381 positively related to the interaction between discharge and stream temperature ( $b = 0.0015$ ,  $p <$   
382  $0.001$ ) (model conditional  $R^2 = 0.62$ , marginal  $R^2 = 0.28$ ). Freshness Index was negatively related  
383 to stream temperature ( $b = -0.003$ ,  $p = 0.008$ ) (model conditional  $R^2 = 0.59$ , marginal  $R^2 = 0.23$ ),  
384 while Fluorescence Index was not significantly related to either discharge or stream temperature.

### 385 **3.4 PARAFAC characterization of DOM**

386 Six fluorescence components were identified through PARAFAC (“C1” through “C6”)  
387 (Table 2). Additional details on PARAFAC model results are provided in Supplemental Table  
388 S4.1, Fig. S4.2, and Fig. S4.3. Of the six components, four were found to have close spectral  
389 matches in the OpenFluor database (C1, C3, C5, C6; minimum similarity score  $> 0.95$ ), while  
390 the remaining two (C2 and C4) were found to have similar peaks represented in the literature.  
391 The first four components (C1 through C4) are described as terrestrial-derived, whereas  
392 components C5 and C6 are described as autochthonous or microbially-derived (Table 2). In  
393 general, the rank order of each components’ percent contribution to total fluorescence was  
394 maintained over time, with C1 comprising the majority of total fluorescence across all  
395 watersheds (Fig. 6).

396 Across watersheds, components fluctuated synchronously over time and variation  
397 between watersheds was relatively low, although slightly more variation between watersheds  
398 was observed during the beginning of the dry period relative to other times of the year (Fig 6).

399 The percent contributions of components C1, C3, C5 and C6 to total fluorescence were not  
400 significantly different across watersheds (for all components Kruskal-Wallis test,  $p > 0.05$ ),  
401 however percent composition of both C2 and C4 were different (Kruskal-Wallis test,  $p = 0.0306$   
402 and  $p = 0.0307$ , respectively) and higher for watersheds 819 and 844 relative to the other  
403 watersheds (Supplemental Fig. S4.4).

404 PARAFAC components exhibited significant relationships with stream discharge and  
405 stream temperature, although predicted changes (beta, or  $b$ ) in fluorescence components with  
406 discharge and/or stream temperature were small (Supplemental Table S6.2). C3 increased with  
407 discharge ( $b = 0.006$ ,  $p = 0.003$ ), whereas C2, C4, and C5 decreased with discharge (C2:  $b = -$   
408  $0.005$ ,  $p = 0.022$ ; C4:  $b = -0.008$ ,  $p = 0.002$ ; C5:  $b = -0.008$ ,  $p = 0.002$ ). C1, C4, and C6 increased  
409 with temperature (C1:  $b = 0.001$ ,  $p = 0.050$ ; C4:  $b = 0.003$ ,  $p < 0.001$ ; C6:  $b = 0.005$ ,  $p = 0.005$ ),  
410 while both C3 and C5 decreased with temperature (C3:  $b = -0.003$ ,  $p = 0.003$ ; C5:  $b = -0.003$ ,  $p =$   
411  $0.027$ ). Conditional  $R^2$  values for the models ranged from 0.28 to 0.69, while marginal  $R^2$  ranged  
412 from 0.20 to 0.46. Overall, greater changes in component contribution to total fluorescence were  
413 observed with changes in discharge relative to changes in stream temperature.

### 414 **3.5 Relationships between watershed characteristics, DOC concentrations, and DOM** 415 **composition**

416 Results of the partial-RDA (type 2 scaling) were significant in explaining variability in  
417 DOM concentration and composition (semi-partial  $R^2 = 0.33$ ,  $F = 7.90$ ,  $p < 0.0001$ ) (Fig. 7). Axes  
418 1 through 3 were statistically significant at  $p < 0.001$ , and the relative contribution of each axis to  
419 the total explained variance was 47%, 30%, and 22%, respectively. Additional details on the  
420 RDA test are provided in Supplemental Figs. S5.1-S5.2 and Tables S5.3 – S5.5. Axis 1 described  
421 a gradient of watershed coverage by water-inundated ecosystem types, ranging from more

422 wetland coverage to more lake coverage. Total lake coverage (area) and mean mineral soil  
423 material thickness showed a strong positive contribution, and wetland coverage (area) showed a  
424 strong negative contribution to this axis. Freshness Index, Fluorescence Index,  $S_R$  and  
425 fluorescence component C6 were positively correlated with Axis 1, while component C4 showed  
426 a clear negative correlation. Axis 2 described a subtler gradient of soil material thickness ranging  
427 from greater mean organic soil material thickness to greater mean mineral soil material  
428 thickness. DOC concentration,  $\delta^{13}\text{C-DOC}$ ,  $\text{SUVA}_{254}$ , and fluorescence component C1 all showed  
429 a strong, positive correlation with Axis 2. Axis 3 described a gradient of watershed steepness,  
430 from lower gradient slopes with more wetland area and thicker organic soil material to steeper  
431 slopes with less developed organic horizons. Average slope contributed negatively to Axis 3 (see  
432 Supplemental Table S5.5), followed by positive contributions from both wetland area and  
433 thickness of organic soil material.  $\delta^{13}\text{C-DOC}$  showed the most positive correlation with Axis 3,  
434 whereas fluorescence components C1 and C4 showed the most negative.

#### 435 **4. Discussion**

##### 436 **4.1 DOC export from small catchments to the coastal ocean**

437 In comparison to previous studies, our estimate of freshwater DOC yields from Calvert  
438 and Hecate Island watersheds are in the upper range predicted for this region based on global  
439 models (Mayorga et al., 2010) and DOC exports quantified for southeastern Alaska (D'Amore et  
440 al., 2015a; D'Amore et al., 2016; Stackpoole et al., 2017). Compared to watersheds of similar  
441 size, DOC yields from Calvert and Hecate Island watersheds are some of the highest observed  
442 (see reviews in Hope et al., 1994; Alvarez-Cobelas et al., 2012), including DOC yields  
443 determined from many tropical rivers, despite the fact that tropical rivers have been shown to  
444 export very high DOC (e.g., Autuna River, Venezuela, DOC yield= 56,946 kg C km<sup>-2</sup> yr<sup>-1</sup>;

445 Castillo et al., 2004), and are often regarded as having disproportionately high carbon export  
446 compared to temperate and Arctic rivers (Aitkenhead and McDowell, 2000; Borges et al., 2015).  
447 Our estimates of DOC yield are comparable to, or higher than, previous estimates from high-  
448 latitude catchments of similar size that receive high amounts of precipitation and contain  
449 extensive organic soils and wetlands (e.g. Naiman, 1982 (DOC yield= 48,380 kg C km<sup>-2</sup> yr<sup>-1</sup>);  
450 Brooks et al., 1999 (DOC yield= 20,300 kg C km<sup>-2</sup> yr<sup>-1</sup>); Ågren et al., 2007 (DOC yield= 32,043  
451 kg C km<sup>-2</sup> yr<sup>-1</sup>)). However, many of these catchments represent low (first or second) order  
452 headwater streams that drain to higher order stream reaches, rather than directly to the ocean.  
453 Although headwater streams have been shown to export up to 90 % of the total annual carbon in  
454 stream systems (Leach et al., 2016), significant processing and loss typically occurs during  
455 downstream transit (Battin et al., 2008).

456 Over much of the incised outer coast of the CTR, small rainfall-dominated catchments  
457 contribute high amounts of freshwater runoff to the coastal ocean (Royer, 1982; Morrison et al.,  
458 2012; Carmack et al., 2015). Small mountainous watersheds that discharge directly to the ocean  
459 can exhibit disproportionately high fluxes of carbon relative to watershed size, and in aggregate  
460 may deliver more than 50% of total carbon flux from terrestrial systems to the ocean (Milliman  
461 and Syvitski, 1992; Masiello and Druffel, 2001). Extrapolating our estimate of annual DOC yield  
462 from Calvert and Hecate Island watersheds to the entire hypermaritime subregion of British  
463 Columbia's CTR (29,935 km<sup>2</sup>), generates an estimated annual DOC flux of 0.997 Tg C yr<sup>-1</sup>  
464 (0.721 to 1.305 Tg C yr<sup>-1</sup> for our lowest to highest yielding watersheds, respectively), with the  
465 caveat that this estimate is rudimentary and does not account for spatial heterogeneity in  
466 controlling factors such as wetland extent, topography, watershed size. Regional comparisons  
467 estimate that Southeast Alaska (104,000 km<sup>2</sup>), at the northern range of the CTR, exports



468 approximately 1.25 Tg C yr<sup>-1</sup> (Stackpoole et al., 2016), while south of the perhumid CTR, the  
469 wet northwestern United States and its associated coastal temperate rainforests export less than  
470 0.153 Tg C yr<sup>-1</sup> as DOC (reported as TOC, Butman et al., 2016). This suggests that the  
471 hypermaritime coast of British Columbia plays an important role in the export of DOC from  
472 coastal temperate rainforest ecosystems of western North America, in a region that is already  
473 expected to contribute high quantities of DOC to the coastal ocean.

#### 474 **4.2. Seasonal variability in DOC export**

475 Despite having an ocean-moderated climate compared to continental interiors, the study  
476 area experiences seasonal patterns in precipitation dominated by a longer wet period and a  
477 shorter, drier period. Flashy stream hydrographs indicate that hydrologic response times for  
478 Calvert and Hecate Island watersheds are rapid, presumably as a result of small catchment size,  
479 high drainage density, and relatively shallow soils with high hydraulic conductivity (Gibson et  
480 al., 2000; Fitzgerald et al., 2003). Rapid runoff is presumably accompanied by rapid increases in  
481 water tables and lateral movement of water through shallow soil layers rich in organic matter  
482 (Fellman et al., 2009b; D'Amore et al., 2015b). During drier periods DOC pools increase in soils  
483 and are flushed to streams when water tables rise (Boyer et al., 1996).

484 Precipitation is a well-established driver of stream DOC export (Alvarez-Cobelas et al.,  
485 2012), particularly in systems containing organic soils and wetlands (Olefeldt et al., 2013; Wallin  
486 et al., 2015; Leach et al., 2016). Frequent, high intensity precipitation events and short residence  
487 times are expected to result in pulsed exports of stream DOC that are rapidly shunted  
488 downstream, thus reducing time for in-stream processing (Raymond et al., 2016). On Calvert and  
489 Hecate Islands, the combination of high rainfall, rapid runoff, and abundant sources of DOC  
490 from organic-rich soils, wetlands, and forests, result in high DOC fluxes. The process of “DOC

491 flushing” has been shown to increase stream water DOC during higher flows in coastal and  
492 temperate watersheds (e.g., Sanderman et al., 2009; Deirmendjian et al., 2017). In our study, the  
493 relationship between DOC concentration and discharge varied by watershed (see Supplemental  
494 Fig. S6.1), but overall DOC concentrations increased with both discharge and temperature. This  
495 indicates that while watershed characteristics are important for influencing the magnitude and  
496 variability of DOC concentrations and export, the hydrologic coupling of precipitation and  
497 discharge with seasonal production and availability of DOC is an overarching driver of DOC  
498 export (Fasching et al., 2016).

#### 499 **4.3 DOM character: Sources and variability**

500 Measures of DOM composition from Calvert and Hecate Islands suggest that carbon and  
501 organic matter exported from these systems is highly terrestrial. Values for  $\delta^{13}\text{C}$ -DOC were  
502 relatively constrained, suggesting terrestrial carbon sources from C3 plants and soils were the  
503 dominant input to catchment stream water DOM (Finlay and Kendall, 2007). Measures of  $S_R$  and  
504  $\text{SUVA}_{254}$  were typical of environments that export large quantities of high molecular weight,  
505 highly aromatic DOM such as some tropical rivers (e.g., Lambert et al., 2016; Mann et al., 2014),  
506 streams draining wetlands (e.g., Ågren et al., 2008, Austnes et al., 2010), or streams draining  
507 small undisturbed catchments comprised of mixed forest and wetlands (e.g. Wickland et al.,  
508 2007; Fellman et al., 2009a; Spencer et al., 2010, Yamashita et al., 2011). This suggests the  
509 majority of the DOM pool is comprised of larger molecules that have not been extensively  
510 chemically or biologically degraded through processes such as microbial utilization or  
511 photodegradation, and therefore are potentially more biologically available (Amon and Benner,  
512 1996).

513           Seasonal variability in DOM composition may be attributed to seasonal changes in  
514 biological activity and shifting flow paths that affect hydrologic interactions with different DOM  
515 source materials (Fellman et al., 2009b). On Calvert and Hecate Island watersheds, some  
516 measures of DOM composition, such as  $\delta^{13}\text{C}$ -DOC and  $S_R$ , exhibited seasonal patterns. In our  
517 study, discharge was significantly related to  $\delta^{13}\text{C}$ -DOC and  $S_R$ , with higher discharge resulting in  
518 more terrestrial-like DOM (i.e., more depleted  $\delta^{13}\text{C}$ -DOC and lower  $S_R$ ) as saturated conditions  
519 promote the mobilization of a wider range of DOM from soil material (McKnight et al., 2001;  
520 Kalbitz et al., 2002). This is similar to findings of Sanderman et al. (2009), who observed distinct  
521 relationships between discharge and both  $\delta^{13}\text{C}$ -DOC and  $\text{SUVA}_{254}$ , and postulated that during  
522 the rainy season, hillslope flushing shifts DOM sources to more aged soil organic material  
523 because plant productivity is not rapid enough to meet microbial demand, forcing microbes to  
524 switch to metabolizing more aged DOM within soils. It has also been shown that rising water  
525 tables can establish strong hydraulic gradients that initiate and sustain prolonged increases in  
526 metrics like  $\text{SUVA}_{254}$ , until the progressive drawdown of upland water tables constrain flow  
527 paths (Lambert et al., 2013).

528           During the drier and warmer period, DOM decreased in molecular weight ( $S_R$ ) and  
529 Freshness Index, as well as increased in C6, a component comprised of protein-like composition.  
530 This suggests a shift in the source of DOM and/or increased contributions from less aromatic,  
531 lower molecular weight material, such as DOM derived from increased terrestrial primary  
532 production (Berggren et al., 2010), and perhaps deeper flow paths that contribute to mineral  
533 binding and export of older, more processed terrestrial material (McKnight et al., 2001; van Hees  
534 et al., 2005). Proportions of fluorescence components were generally consistent across  
535 watersheds during the dry period, but diverged during the wet period, further suggesting that

536 water table draw down and unsaturated soils lead to more diverse flow paths and hydrologic  
537 interaction with different sources of DOM.

538         Interestingly, more depleted values of  $\delta^{13}\text{C}$ -DOC were also related to warmer  
539 temperature. The positive relationship between  $\delta^{13}\text{C}$ -DOC and both discharge and temperature,  
540 as well as the overall low variability in  $\delta^{13}\text{C}$ -DOC, suggests that the availability or production of  
541 terrestrial DOM is enough to keep up with microbial demand, allowing the supply of terrestrial  
542 material to remain relatively seasonally consistent. The positive relationship of temperature and  
543 Freshness Index, as well as with C1 and C4, further suggests that warmer periods contribute to a  
544 fresh supply of terrestrial material available for microbial degradation and export (Fellman et al.,  
545 2009a; Fasching et al., 2016).

546         The interaction of sources and flow paths during wet versus dry periods may have  
547 important consequences for the downstream fate of this material. For example, biological  
548 utilization of DOM is influenced by its composition (e.g. Judd et al., 2006; Fasching et al.,  
549 2014), therefore differences in the nature of DOM exports will likely alter the downstream fate  
550 and ecological role of freshwater-exported DOM. The majority of the fluorescent DOM pool was  
551 comprised of C1, which is described as humic-like, less-processed terrestrial soil and plant  
552 material (see Table 2). This may represent a relatively fresh, seasonally-consistent contribution  
553 of terrestrial subsidy from streams to the coastal ecosystem, which is relatively lower in carbon  
554 and nutrients throughout much of the year (Whitney et al., 2005; Johannessen et al., 2008). For  
555 example, pulsed contributions of less-processed humic material exported from rivers to lakes  
556 have been shown to stimulate bacterial production (Bergström and Jansson, 2000). While  
557 previous studies have suggested that bacteria prefer autochthonous carbon sources, they readily  
558 utilize allochthonous terrestrial DOC subsidies (Bergström and Jansson, 2000; Kritzberg et al.,

2004; McCallister and Giorgio, 2008; Berggren et al., 2010), enabling humic and fulvic material to fuel a low but continuous level of bacterial productivity after more labile sources have been consumed (Guillamette and Giorgio, 2011). In addition, although the tryptophan-like component C6, represents a minor, more variable proportion of total fluorescence in comparison to the more humic compounds such as C1, even a small proteinaceous fraction of the overall DOM pool can play a major role in overall bioavailability and bacterial utilization of DOM (Berggren et al., 2010; Guillamette and Giorgio, 2011).

#### 4.4 Relationships between watershed attributes and exported DOM

Previous studies have implicated wetlands as a major driver of DOM composition (e.g., Xenopoulos et al., 2003; Ågren et al., 2008; Creed et al., 2008), however the analysis of relationships between Calvert and Hecate Island landscape attributes and variation in DOM composition suggests that controls on DOM composition are more nuanced than being solely driven by the presence of wetlands. Ågren et al. (2008) found that when wetland area comprised >10% of total catchment area, wetland DOM was the most significant driver of stream DOM composition during periods of high hydrologic connectivity. Although wetlands comprise an average of 37% of our study area, they do not appear to be the single leading driver of variability in DOC concentration and DOM composition. Other factors, such as watershed slope, the depth of organic and mineral soil materials, and the presence of lakes also appear to influence DOC concentration and DOM composition.

In these watersheds, soils with pronounced accumulations of organic matter are not restricted to wetland ecosystems. Peat accumulation in wetland ecosystems results in the formation of organic soils (Hemists), where mobile fractions of DOM accumulate under saturated soil conditions and limited drainage, resulting in the enrichment of poorly

582 biodegradable, more stable humic acids (Stevenson, 1994; Marschner and Kalbitz, 2003).  
583 Although Hemist soils comprise 27.8% of our study area, Follic Histosols, which form under  
584 more freely drained conditions, such as steeper slopes, occur over an additional 25.7% of the  
585 region (Supplemental S1.2). In freely drained organic soils, high rates of respiration can result in  
586 further enrichment of aromatic and more complex molecules, and this material may be rapidly  
587 mobilized and exported to streams (Glatzel et al., 2003). This suggests the importance of widely  
588 distributed, alternative soil DOM source-pools, such as Follic Histosols and associated Podzols  
589 with thick forest floors on hillslopes, available to contribute high amounts of terrestrial carbon  
590 for export.

591         Although lakes make up a relatively small proportion of the total landscape area, their  
592 influence on DOM export appears to be important. The proportion of lake area can be a good  
593 predictor of organic carbon loss from a catchment since lakes often increase hydrologic  
594 residence times and thus increase opportunities for biogeochemical processing (Algesten et al.,  
595 2004; Tranvik et al., 2009). In our study, watersheds with a larger percentage of lake area  
596 exhibited slower response following rain events (Supplemental Fig. S2.2), lower DOC yields,  
597 and lake area was correlated with parameters that represent greater autochthonous DOM  
598 production or microbial processing such as higher Freshness Index,  $S_R$ , Fluorescence Index, and  
599 higher proportions of component C6. In contrast, watersheds with a high percentage of wetlands  
600 contributed DOM that was more allochthonous in composition. Lakes are known to be important  
601 landscape predictors of DOC, as increased residence time enables removal via respiration, thus  
602 reducing downstream exports from lake outlets (Larson et al., 2007). The proximity of wetlands  
603 and lakes within the catchment and their proximity to the watershed outlet can also play an  
604 important role in the composition of DOM exports (Martin et al., 2006).

## 605 **5. Conclusions**

606 Previous work has demonstrated freshwater discharge is substantial along the coastal  
607 margin of the North Pacific temperate rainforest, and plays an important role in processes such as  
608 ocean circulation (Royer, 1982; Eaton and Moore, 2010). Our finding that small catchments in  
609 this region contribute high yields of terrestrial DOC to coastal waters suggests that freshwater  
610 inputs may also influence ocean biogeochemistry and food web processes through terrestrial  
611 organic matter subsidies. Our findings also suggest that this region may be currently  
612 underrepresented in terms of its role in global carbon cycling. Currently, there is no region-wide  
613 carbon flux model for the Pacific coastal temperate rainforest or the greater Gulf of Alaska,  
614 which would quantify the importance of this region within the global carbon budget. Our  
615 estimates represent the hypermaritime outer-coast zone of the CTR, where subdued terrain, high  
616 rainfall, ocean moderated temperatures and poor bedrock have generated a distinctive ‘bog-  
617 forest’ landscape mosaic within the greater temperate rainforest (Banner et al. 2005). Even  
618 within our geographically limited study area, we observed a range of DOC yields across  
619 watersheds. To quantify regional scale fluxes of rainforest carbon to the coastal ocean, further  
620 research will be needed to estimate DOC yields across complex spatial gradients of topography,  
621 climate, hydrology, soils and vegetation. Long term changes in DOC flux have been observed in  
622 many places (e.g., Worrall et al., 2004; Borken et al., 2011; Lepistö et al., 2014; Tank et al.,  
623 2016) and continued monitoring of this system will allow us to better understand the underlying  
624 drivers of export and evaluate future patterns in DOC yields. Coupled with current studies  
625 investigating the fate of terrestrial material in ocean food webs, this work will improve our  
626 understanding of coastal carbon patterns, and increase capacity for predictions regarding the  
627 ecological impacts of climate change.

628 **Author Contributions**

629 The authors declare that they have no conflict of interest.

630 A.A. Oliver prepared the manuscript with contributions from all authors, designed analysis  
631 protocols, analyzed samples, performed the modeling and analysis for dissolved organic carbon  
632 fluxes, parallel factor analysis of dissolved organic matter composition, and all remaining  
633 statistical analyses. S.E. Tank assisted with designing the study and overseeing laboratory  
634 analyses, crafting the scope of the paper, and determining the analytical approach.

635 I. Giesbrecht led the initial DOC sampling design, helped coordinate the research team, oversaw  
636 routine sampling and data management, and led the watershed characterization.

637 M.C. Korver developed the rating curves, and conducted the statistical analysis of discharge  
638 measurement uncertainties and rating curve uncertainties. W.C. Floyd lead the hydrology  
639 component of this project, selected site locations, installed and designed the hydrometric  
640 stations, and developed the rating curves and final discharge calculations. C. Bulmer and P.  
641 Sanborn collected and analyzed soil field data and prepared the digital soils map of the  
642 watersheds. K.P. Lertzman conceived of and co-led the overall study of which this paper is a  
643 component, helped assemble and guide the team of researchers who carried out this work,  
644 provided input to each stage of the study.

645

646 **Acknowledgements**

647 This work was funded by the Tula Foundation and the Hakai Institute. The authors would like to  
648 thank many individuals for their support, including Skye McEwan, Bryn Fedje, Lawren McNab,  
649 Nelson Roberts, Adam Turner, Emma Myers, David Norwell, and Chris Coxson for sample  
650 collection and data management, Clive Dawson and North Road Analytical for sample



651 processing and data management, Keith Holmes for creating our maps, Matt Foster for database  
652 development and support, Shawn Hateley for sensor network maintenance, Jason Jackson, Colby  
653 Owen, James McPhail, and the entire staff at Hakai Energy Solutions for installing and  
654 maintaining the sensors and telemetry network, and Stewart Butler and Will McInnes for field  
655 support. Thanks to Santiago Gonzalez Arriola for generating the watershed summaries and  
656 associated data products, and Ray Brunsting for overseeing the design and implementation of the  
657 sensor network and the data management system at Hakai. Additional thanks to Lori Johnson  
658 and Amelia Galuska for soil mapping field assistance, and Francois Guillet for PARAFAC  
659 consultation. Thanks to Dave D'Amore for inspiring the Hakai project to investigate aquatic  
660 fluxes at the coastal margin and for technical guidance. Lastly, thanks to Eric Peterson and  
661 Christina Munck who provided significant guidance throughout the process of designing and  
662 implementing this study.

663

## 664 **References**

665 Ågren, A., Buffam, I., Jansson, M. and Laudon, H.: Importance of seasonality and small streams  
666 for the landscape regulation of dissolved organic carbon export, *J. Geophys. Res. Biogeosci.*,  
667 112(G3), doi:10.1029/2006JG000381, 2007.

668

669 Ågren, A., Buffam, I., Berggren, M., Bishop, K., Jansson, M. and Laudon, H.: Dissolved organic  
670 carbon characteristics in boreal streams in a forest-wetland gradient during the transition  
671 between winter and summer, *J. Geophys. Res. Biogeosci.*, 113(G3), doi:10.1029/2007JG000674,  
672 2008.

673

674 Akaike, H.: Likelihood of a model and information criteria, *J. Econometrics*, 16(1), 3-14,  
675 doi:10.1016/0304-4076(81)90071-3, 1981.

676

677 Aitkenhead, J.A., and McDowell, W.H.: Soil C:N ratio as a predictor of annual riverine DOC  
678 flux at local and global scales, *Global Biogeochem. Cycles*, 14(1), 127–138,  
679 doi:10.1029/1999GB900083, 2000.

680

681 Alaback, P.B.: Biodiversity patterns in relation to climate: The coastal temperate rainforests of  
682 North America, *Ecol. Stud.*, 116, 105–133, doi:10.1007/978-1-4612-3970-3\_7, 1996.  
683

684 Algesten, G., Sobek, S., Bergström, A., Ågren, A., Tranvik, L. and Jansson, M.: Role of lakes for  
685 organic carbon cycling in the boreal zone, *Global Change Biol.*, 10(1), 141–147,  
686 doi:10.1111/j.1365-2486.2003.00721.x, 2004.  
687

688 Alvarez-Cobelas, M., Angeler, D., Sánchez-Carrillo, S. and Almendros, G.: A worldwide view  
689 of organic carbon export from catchments, *Biogeochemistry*, 107(1-3), 275–293,  
690 doi:10.1007/s10533-010-9553-z, 2012.  
691

692 Amon, R.M.W., and Benner, R.: Bacterial utilization of different size classes of dissolved  
693 organic matter, *Limnol. Oceanogr.*, 41, 41-51, 1996.  
694

695 Aufdenkampe, A., Mayorga, E., Raymond, P., Melack, J., Doney, S., Alin, S., Aalto, R., and  
696 Yoo, K.: Riverine coupling of biogeochemical cycles between land, oceans, and atmosphere,  
697 *Front. Ecol. Environ.*, 9(1), 53–60, doi:10.1890/100014, 2011.  
698

699 Austnes, K., Evans, C.D., Eliot-Laize, C., Naden, P.S., and Old, G.H.: Effects of storm events on  
700 mobilisation and in-stream processing of dissolved organic matter (DOM) in a Welsh peatland  
701 catchment, *Biogeochem.*, 99, 157-173, doi:10.1007/s10533-009-9399-4, 2010.  
702

703 Banner, A., LePage, P., Moran, J., and de Groot, A. (Eds.): The HyP3 Project: pattern,  
704 process, and productivity in hypermaritime forests of coastal British Columbia -  
705 a synthesis of 7-year results, Special Report 10, Res. Br., British Columbia Ministry Forests,  
706 Victoria, British Columbia, 142 pp., available at:  
707 <http://www.for.gov.bc.ca/hfd/pubs/Docs/Srs/Srs10.htm>, 2005.  
708

709 Battin, T.J., Kaplan, L.A., Findlay, S., Hopkinson, C.S., Marti, E., Packman, A.I., Newbold, D.,  
710 and Sabater, F.: Biophysical controls on organic carbon fluxes in fluvial networks, *Nature*  
711 *Geosci.*, 1, 95–100, 2008.  
712

713 Bauer, J.E., Cai, W.J., Raymond, P.A., T.S., Bianchi, Hopkinson, C.S., and Regnier, P.A.G.: The  
714 changing carbon cycle of the coastal ocean, *Nature*, 504(7478), 61-70, doi:10.1038/nature12857,  
715 2013.  
716

717 Berggren, M., Laudon, H., Haei, M., Ström, L., and Jansson, M.: Efficient aquatic bacterial  
718 metabolism of dissolved low-molecular-weight compounds from terrestrial sources, *ISME J.*,  
719 doi:10.1038/ismej.2009.120, 2010.  
720

721 Bergström, A.K., and Jansson, M.: Bacterioplankton production in humic Lake Örträsket in  
722 relation to input of bacterial cells and input of allochthonous organic carbon, *Microb. Ecol.*,  
723 doi:10.1007/s002480000007, 2000.  
724

725 Boehme, J. and Coble, P.: Characterization of Colored Dissolved Organic Matter Using High-  
726 Energy Laser Fragmentation, *Environ. Sci. Technology*, 34(15), 3283–3290,  
727 doi:10.1021/es9911263, 2000.  
728

729 Borcard, D., Gillet, F., and Legendre, P.: *Numerical ecology with R*, Springer, New York,  
730 United States, doi:10.1007/978-1-4419-7976-6, 2011.  
731

732 Borken, W., Ahrens, B., Schultz, C. and Zimmermann, L.: Site-to-site variability and temporal  
733 trends of DOC concentrations and fluxes in temperate forest soils, *Global Change Biol.*, 17:  
734 2428–2443, doi:10.1111/j.1365-2486.2011.02390.x, 2011.  
735

736 Borges, A.V., Darchambeau, F., Teodoru, C.R., Marwick, T.R., Tamooh, F., Geeraert, N.,  
737 Omengo, F.O., Guérin, F., Lambert, T., Morana, C., Okuku, E., and Bouillon, S.: Globally  
738 significant greenhouse-gas emissions from African inland waters, *Nature Geosci.*, 8, 637–642,  
739 doi:10.1038/ngeo2486, 2015.  
740

741 Boyer, E.W., Hornberger, G.M., Bencala, K.E., and McKnight, D.: Overview of a simple model  
742 describing variation of dissolved organic carbon in an upland catchment, *Ecol. Modell.*, 86, 183-  
743 188, 1996.  
744

745 Burnham K.P., and Anderson, D.R.: *Model selection and multimodel inference*, 2nd edn.  
746 Springer, New York, 2002.  
747

748 Carmack, E., Winsor, P., and William, W.: The contiguous panarctic Riverine Coastal Domain:  
749 A unifying concept, *Prog. Oceanogr.*, 139, 13-23, doi:10.1016/j.pocean.2015.07.014, 2015.  
750

751 Castillo, M.M., Allan, J.D., Sinsabaugh, R.L., and Kling, G.W.: Seasonal and interannual  
752 variation of bacterial production in lowland rivers of the Orinoco basin, *Freshwater Biol.*, 49(11),  
753 1400-1414, doi:10.1111/j.1365-2427.2004.01277.x, 2004.  
754

755 Clark, J.M., Lane, S.N., Chapman, P.J., and Adamson, J.K.: Export of dissolved organic carbon  
756 from an upland peatland during storm events: Implications for flux estimates, *J. Hydrol.*, 347(3-  
757 4), 438-447, doi: 10.1016/j.jhydrol.2007.09.030, 2007.  
758

759 Coble, P., Castillo, C. and Avril, B.: Distribution and optical properties of CDOM in the Arabian  
760 Sea during the 1995 Southwest Monsoon, *Deep Sea Res. Part II, Oceanogr.*, 45(10-11), 2195–  
761 2223, doi:10.1016/S0967-0645(98)00068-X, 1998.  
762

763 Cole, J., Prairie, Y., Caraco, N., McDowell, W., Tranvik, L., Striegl, R., Duarte, C., Kortelainen,  
764 P., Downing, J., Middelburg, J. and Melack, J.: Plumbing the Global Carbon Cycle: Integrating  
765 Inland Waters into the Terrestrial Carbon Budget, *Ecosystems*, 10(1), 172–185,  
766 doi:10.1007/s10021-006-9013-8, 2007.  
767

768 Cory, R.M., and McKnight, D.M.: Fluorescence spectroscopy reveals ubiquitous presence of  
769 oxidized and reduced quinines in dissolved organic matter, *Environ. Sci. Technol.*, 39, 8142 -  
770 8149, doi:10.1021/es0506962, 2005.

771  
772 Creed, I.F., Beall, F.D., Clair, T.A., Dillon, P.J., and Hesslein, R.H.: Predicting export of  
773 dissolved organic carbon from forested catchments in glaciated landscapes with shallow soils,  
774 *Glob. Biogeochem. Cycles*, 22, GB4024, doi:10.1029/2008GB003294, 2008.  
775  
776 D'Amore, D.V., Edwards, R.T., and Biles, F.E.: Biophysical controls on dissolved organic  
777 carbon concentrations of Alaskan coastal temperate rainforest streams, *Aquat. Sci.*,  
778 doi:10.1007/s00027-015-0441-4, 2015a.  
779  
780 D'Amore, D.V., Edwards, R.T., Herendeen, P.A., Hood, E., and Fellman, J.B.: Dissolved  
781 organic carbon fluxes from hydrogeologic units in Alaskan coastal temperate rainforest  
782 watersheds, *Soil Sci. Soc. Am. J.*, 79:378-388, doi:10.2136/sssaj2014.09.0380, 2015b.  
783  
784 D'Amore, D.V., Biles, F.E., Nay, M., Rupp, T.S.: Watershed carbon budgets in the southeastern  
785 Alaskan coastal forest region, in: *Baseline and projected future carbon storage and greenhouse-*  
786 *gas fluxes in ecosystems of Alaska*, U.S. Geological Survey Professional Paper, 1826, 196 p.,  
787 2016.  
788  
789 Dai, M., Yin, Z., Meng, F., Liu, Q. and Cai, W.J.: Spatial distribution of riverine DOC inputs to  
790 the ocean: an updated global synthesis, *Curr. Opin. Sust.*, 4(2), 170–178,  
791 doi:10.1016/j.cosust.2012.03.003, 2012.  
792  
793 Deirmendjian, L., Loustau, D., Augusto, L., Lafont, S., Chipeaux, C., Poirier, D., and Abril, G.:  
794 Hydrological and ecological controls on dissolved carbon concentrations in groundwater and  
795 carbon export to surface waters in a temperate pine forest watershed, *Biogeosciences*  
796 *Discuss.*, doi:10.5194/bg-2017-90, in review, 2017.  
797  
798 DellaSala, D.A.: *Temperate and Boreal Rainforests of the World*, Island Press, Washington,  
799 D.C., 2011.  
800  
801 Emili, L. and Price, J.: Biogeochemical processes in the soil-groundwater system of a forest-  
802 peatland complex, north coast British Columbia, Canada, *Northwest Sci.*, 88, 326–348,  
803 doi:10.3955/046.087.0406, 2013.  
804  
805 Fasching, C., Behounek, B., Singer, G. and Battin, T.: Microbial degradation of terrigenous  
806 dissolved organic matter and potential consequences for carbon cycling in brown-water streams,  
807 *Sci. Rep.*, 4, 4981, doi:10.1038/srep04981, 2014.  
808  
809 Fasching, C., Ulseth, A., Schelker, J., Steniczka, G. and Battin, T.: Hydrology controls dissolved  
810 organic matter export and composition in an Alpine stream and its hyporheic zone, *Limnol.*  
811 *Oceanogr.*, 61(2), 558–571, doi:10.1002/lno.10232, 2016.  
812  
813 Fellman, J., Hood, E., D'Amore, D., Edwards, R. and White, D.: Seasonal changes in the  
814 chemical quality and biodegradability of dissolved organic matter exported from soils to streams  
815 in coastal temperate rainforest watersheds, *Biogeochemistry*, 95, 277–293, doi:10.1007/s10533-  
816 009-9336-6, 2009a.

817  
818 Fellman, J., Hood, E., Edwards, R. and D'Amore, D.: Changes in the concentration,  
819 biodegradability, and fluorescent properties of dissolved organic matter during stormflows in  
820 coastal temperate watersheds, *J. Geophys. Res. Biogeosci.*, 114, doi:10.1029/2008JG000790,  
821 2009b.  
822  
823 Fellman, J., Hood, E. and Spencer, R.: Fluorescence spectroscopy opens new windows into  
824 dissolved organic matter dynamics in freshwater ecosystems: A review, *Limnol. Oceanogr.*, 55,  
825 24522462, doi:10.4319/lo.2010.55.6.2452, 2010.  
826  
827 Fellman, J., Nagorski, S., Pyare, S., Vermilyea, A.W., Scott, D., and Hood, E.: Stream  
828 temperature response to variable glacier cover in coastal watersheds of Southeast Alaska,  
829 *Hydrol. Process.*, 28, 2062-2073, doi:10.1002/hyp.9742, 2014  
830  
831 Finlay, J.C., and Kendall, C.: Stable isotope tracing of temporal and spatial variability in organic  
832 matter sources and variability in organic matter sources to freshwater ecosystems, in *Stable*  
833 *Isotopes in Ecology and Environmental Science*, 2, Michener, R., and Lajtha, K. (Eds),  
834 Blackwell Publishing Ltd, Oxford, UK, 283-324, 2007.  
835  
836 Fitzgerald, D., Price, J., and Gibson, J.: Hillslope-swamp interactions and flow pathways in a  
837 hypermaritime rainforest, British Columbia, *Hydrol. Process.*, 17, 3005-3022,  
838 doi:10.1002/hyp.1279, 2003.  
839  
840 Gibson, J.J., Price, J.S., Aravena, R., Fitzgerald, D.F., and Maloney, D.: Runoff generation in a  
841 hypermaritime bog-forest upland, *Hydrol. Process*, 14, 2711-2730, doi: 10.1002/1099-  
842 1085(20001030)14:15<2711::AID-HYP88>3.0.CO;2-2, 2000.  
843  
844 Glatzel, S., Kalbitz, K., Dalva, M., and Moore, T.: Dissolved organic matter properties and their  
845 relationship to carbon dioxide efflux from restored peat bogs, *Geoderma*, 113, 397-411, 2003.  
846  
847 Gonzalez Arriola S., Frazer, G.W., Giesbrecht, I.: LiDAR-derived watersheds and their metrics  
848 for Calvert Island, Hakai Institute, doi:dx.doi.org/10.21966/1.15311, 2015.  
849  
850 Gorham, E., Lehman, C., Dyke, A., Clymo, D., and Janssens, J.: Long-term carbon sequestration  
851 in North American peatlands, *Quat. Sci. Review*, 58, 77-82, 2012.  
852  
853 Graeber, D., Gelbrecht, J., Pusch, M., Anlanger, C. and von Schiller, D.: Agriculture has  
854 changed the amount and composition of dissolved organic matter in Central European headwater  
855 streams, *Sci. Total Environ.*, 438, 435-446, doi:10.1016/j.scitotenv.2012.08.087, 2012.  
856  
857 Green, R.N.: Reconnaissance level terrestrial ecosystem mapping of priority landscape units of  
858 the coast EBM planning area: Phase 3, Prepared for British Columbia Ministry Forests, Lands  
859 and Natural Resource Ops., Blackwell and Associates, Vancouver, Canada, 2014.  
860

861 Guillemette, F. and Giorgio, P.: Reconstructing the various facets of dissolved organic carbon  
862 bioavailability in freshwater ecosystems, *Limnol. Oceanogr.*, 56, 734–748,  
863 doi:10.4319/lo.2011.56.2.0734, 2011.

864

865 Hansen, A.M., Kraus, T.E.C., Pellerin, B.A., Fleck, J.A., Downing, B.D., and Bergamaschi,  
866 B.A.: Optical properties of dissolved organic matter (DOM): Effects of biological and photolytic  
867 degradation, *Limnol. Oceanogr.*, 61, 1015-1032, doi:10.1002/lno.10270, 2016.

868

869 Harrell, F.E., Dupont, C., and many others.: Hmisc: Harrell Miscellaneous. R package version  
870 4.0-2. <https://CRAN.R-project.org/package=Hmisc>, 2016.

871

872 Harrison, J., Caraco, N. and Seitzinger, S.: Global patterns and sources of dissolved organic  
873 matter export to the coastal zone: Results from a spatially explicit, global model, *Global*  
874 *Biogeochem. Cycles*, 19, doi:10.1029/2005gb002480, 2005.

875

876 Helms, J., Stubbins, A., Ritchie, J., Minor, E., Kieber, D. and Mopper, K.: Absorption spectral  
877 slopes and slope ratios as indicators of molecular weight, source, and photobleaching of  
878 chromophoric dissolved organic matter, *Limnol. Oceanogr.*, 53, 955–969,  
879 doi:10.4319/lo.2008.53.3.0955, 2008.

880

881 Helton, A., Wright, M., Bernhardt, E., Poole, G., Cory, R. and Stanford, J.: Dissolved organic  
882 carbon lability increases with water residence time in the alluvial aquifer of a river floodplain  
883 ecosystem, *J. Geophys. Res. Biogeosciences*, 120, 693–706, doi:10.1002/2014JG002832, 2015.

884

885 Hoffman, K.M., Gavin, D.G., Lertzman, K.P., Smith, D.J., and Starzomski, B.M.: 13,000 years  
886 of fire history derived from soil charcoal in a British Columbia coastal temperate rain forest,  
887 *Ecosphere*, 7, e01415, doi:10.1002/ecs2.1415, 2016.

888

889 Hope, D., Billett, M.F., and Cresser, M.S.: A review of the export of carbon in river water:  
890 Fluxes and processes, *Environ. Pollut.*, 84(3), 301-324, doi:10.1016/0269-7491(94)90142-2,  
891 1994.

892

893 Hopkinson, C.S., Buffam, I., Hobbie, J., Vallino, J. and Perdue, M.: Terrestrial inputs of organic  
894 matter to coastal ecosystems: An intercomparison of chemical characteristics and bioavailability,  
895 *Biogeochemistry*, 43, 211–234, 1998.

896

897 Hudson, N., Baker, A. and Reynolds, D.: Fluorescence analysis of dissolved organic matter in  
898 natural, waste and polluted waters-a review, *River Res. Appl.*, 23, 631–649,  
899 doi:10.1002/rra.1005, 2007.

900

901 Hurvich, C.M., and Tsai, C.: Regression and time series model selection in small samples,  
902 *Biometrika*, 76(2), 297-307, doi:10.2307/2336663, 1989.

903

904 International Union of Soil Sciences (IUSS) Working Group: World Reference Base for Soil  
905 Resources, International soil classification system for naming soils and creating legends for soil

906 maps, World Soil Resources Reports No. 106, Food and Agricultural Organization of the United  
907 Nations, Rome, Italy, 2015.  
908  
909 ISO Standard 9196: Liquid flow measurement in open channels - Flow measurements under ice  
910 conditions, International Organization for Standardization, available online at [www.iso.org](http://www.iso.org),  
911 1992.  
912  
913 ISO Standard 748: Hydrometry - Measurement of liquid flow in open channels using current-  
914 meters or floats, International Organization for Standardization, available online at [www.iso.org](http://www.iso.org),  
915 2007.  
916  
917 Johannessen, S.C., Potentier, G., Wright, C.A., Masson, D., and Macdonald, R.W.: Water  
918 column organic carbon in a Pacific marginal sea (Strait of Georgia, Canada), *Mar. Environ. Res.*,  
919 66, S49-S61, doi:10.1016/j.marenvres.2008.07.008, 2008.  
920  
921 Johnson, P.C.D.: Extension of Nakagawa & Schielzeth's  $R^2_{GLMM}$  to random slopes models.  
922 *Methods Ecol. Evol.*, DOI: 10.1111/2041-210X.12225, 2014.  
923  
924 Johnson, M., Couto, E., Abdo, M. and Lehmann, J.: Fluorescence index as an indicator of  
925 dissolved organic carbon quality in hydrologic flowpaths of forested tropical watersheds,  
926 *Biogeochemistry*, 105, 149–157, doi:10.1007/s10533-011-9595-x, 2011.  
927  
928 Judd, K., Crump, B. and Kling, G.: Variation in dissolved organic matter controls bacterial  
929 production and community composition, *Ecology*, 87, 2068–2079, doi:10.1890/0012-  
930 9658(2006)87[2068:VIDOMC]2.0.CO;2, 2006.  
931  
932 Kalbitz, K., Schmerwitz, J., Schwesig, D. and Matzner, E.: Biodegradation of soil-derived  
933 dissolved organic matter as related to its properties, *Geoderma*, 113, 273–291,  
934 doi:10.1016/S0016-7061(02)00365-8, 2003.  
935  
936 Kling, G., Kipphut, G., Miller, M. and O'Brien, W.: Integration of lakes and streams in a  
937 landscape perspective: the importance of material processing on spatial patterns and temporal  
938 coherence, *Freshwater Biol.*, 43, 477–497, doi:10.1046/j.1365-2427.2000.00515.x, 2000.  
939  
940 Koehler, A.-K., Murphy, K., Kiely, G. and Sottocornola, M.: Seasonal variation of DOC  
941 concentration and annual loss of DOC from an Atlantic blanket bog in South Western Ireland,  
942 *Biogeochemistry*, 95, 231–242, doi:10.1007/s10533-009-9333-9, 2009.  
943  
944 Lakowicz, J.R.: *Principles of Fluorescence Spectroscopy*, 2, Kluwer Academic, New York,  
945 1999.  
946  
947 Larson, J.H., Frost, P.C., Zheng, Z., Johnston, C.A., Bridgham, S.D., Lodge, D.M., and  
948 Lamberti, G.A.: Effects of upstream lakes on dissolved organic matter in streams, *Limnol.*  
949 *Oceanogr.*, 52(1), 60-69, doi:10.4319/lo.2007.52.1.0060, 2007.  
950

951 Leighty, W.W., Hamburg, S.P., and Caouette, J.: Effects of management on carbon sequestration  
952 in forest biomass in Southeast Alaska, *Ecosystems*, 9, 1051, doi:10.1007/s10021-005-0028-3,  
953 2006.

954

955 Kritzberg, E.S., Cole, J.J. and Pace, M.L.: Autochthonous versus allochthonous carbon sources  
956 of bacteria: Results from whole-lake  $^{13}\text{C}$  addition experiments, *Limnol. Oceanogr.*, 49, 588-596,  
957 doi:10.4319/lo.2004.49.2.0588, 2004.

958

959 Lalonde, K., Middlestead, P., Gélinas, Y.: Automation of  $^{13}\text{C}/^{12}\text{C}$  ratio measurement for  
960 freshwater and seawater DOC using high temperature combustion, *Limnol. Oceanogr. Methods*,  
961 12, 816-829, doi:10.4319/lom.2014.12.816, 2014.

962

963 Lambert, T., Bouillon, S., Darchambeau, F., Massicotte, P., and Borges, A.V.: Shift in the  
964 chemical composition of dissolved organic matter in the Congo River network, *Biogeosci.*, 13,  
965 5405-5420, doi:10.5194/bg-13-5405-2016, 2016.

966

967 Leach, J., Larsson, A., Wallin, M., Nilsson, M. and Laudon, H.: Twelve year interannual and  
968 seasonal variability of stream carbon export from a boreal peatland catchment, *J. Geophys. Res.*  
969 121, 1851–1866, doi:10.1002/2016JG003357, 2016.

970

971 Legendre, P., and Durand, S.: rdaTest, Canonical redundancy analysis, R package version 1.11,  
972 available at <http://adn.biol.umontreal.ca/~numerica/ecology/Rcode/>, 2014.

973

974 Lepistö, A., Futter, M.N. and Kortelainen, P.: Almost 50 years of monitoring shows that climate,  
975 not forestry, controls long-term organic carbon fluxes in a large boreal watershed, *Glob. Change*  
976 *Biol.*, 20, 1225–1237, doi:10.1111/gcb.12491, 2014.

977

978 Liaw, A., and Wiener, M.: Classification and Regression by randomForest, *R News*, 2(3), 18-22,  
979 2002.

980

981 Lochmuller, C.H., Saavedra, S.S.: Conformational changes in a soil fulvic acid measured by time  
982 dependent fluorescence depolarization, *Anal. Chem.*, 38, 1978-1981, 1986.

983

984 Lorenz, D., Runkel, R., and De Cicco, L.: rloadest, River Load Estimation, R package version  
985 0.4.2, available at <https://github.com/USGS-R/rloadest>, 2015.

986

987 Ludwig, W., Probst, J. and Kempe, S.: Predicting the oceanic input of organic carbon by  
988 continental erosion, *Global Biogeochem. Cycles*, 10, 23–41, doi:10.1029/95GB02925, 1996.

989

990 Mann, P.J., Spencer, R.G.M., Dinga, B.J., Poulsen, J.R., Hernes, P.J., Fiske, G., Salter, M.E.,  
991 Wang, Z.A., Hoering, K.A., Six, J., and Holmes, R.M.: The biogeochemistry of carbon across a  
992 gradient of streams and rivers within the Congo Basin, *J. Geophys. Res. Biogeosci.*, 119, 687-  
993 702, doi:10.1002/2013JG002442, 2014.

994



995 Marschner, B., and Kalbitz, K.: Controls on bioavailability and biodegradability of dissolved  
 996 organic matter in soils, *Geoderma*, 113, 211–235, 2003.  
 997  
 998 Martin, S.L., and Soranno, P.A.: Lake landscape position: Relationships to hydrologic  
 999 connectivity and landscape features, *Limnol. Oceanogr.*, 51(2), 801-814,  
 1000 doi:10.4319/lo.2006.51.2.0801, 2006.  
 1001  
 1002 Masiello, C.A., and Druffel, E.R.M.: Carbon isotope geochemistry of the Santa Clara River,  
 1003 *Global Biogeochem. Cycles*, 15, 407-416, doi:10.1029/2000GB001290, 2001.  
 1004  
 1005 Mayorga, E., Seitzinger, S., Harrison, J., Dumont, E., Beusen, A., Bouwman, A.F., Fekete, B.,  
 1006 Kroeze, C. and Drecht, G.: Global Nutrient Export from WaterSheds 2 (NEWS 2): Model  
 1007 development and implementation, *Environ. Model. Softw.*, 25, 837–853,  
 1008 doi:10.1016/j.envsoft.2010.01.007, 2010.  
 1009  
 1010 McCallister, L. S. and Giorgio, P. A.: Direct measurement of the  $\delta^{13}\text{C}$  signature of carbon  
 1011 respired by bacteria in lakes: Linkages to potential carbon sources, ecosystem baseline  
 1012 metabolism, and  $\text{CO}_2$  fluxes, *Limnol. Oceanogr.*, 53, 1204, doi:10.4319/lo.2008.53.4.1204,  
 1013 2008.  
 1014  
 1015 McClelland, J., Townsend-Small, A., Holmes, R., Pan, F., Stieglitz, M., Khosh, M. and Peterson,  
 1016 B.: River export of nutrients and organic matter from the North Slope of Alaska to the Beaufort  
 1017 Sea, *Water Resour. Res.*, 50, 1823–1839, doi:10.1002/2013WR014722, 2014.  
 1018  
 1019 McKnight, D., Boyer, E., Westerhoff, P., Doran, P., Kulbe, T. and Andersen, D.:  
 1020 Spectrofluorometric characterization of dissolved organic matter for indication of precursor  
 1021 organic material and aromaticity, *Limnol. Oceanogr.*, 46, 38–48, doi:10.4319/lo.2001.46.1.0038,  
 1022 2001.  
 1023  
 1024 McLaren, D., Fedje, D., Hay, M.B., Mackie, Q., Walker, I.J., Shugar, D.H., Eamer, J.B.R., Lian,  
 1025 O.B., and Neudorf, C.: A post-glacial sea level hinge on the central Pacific coast of Canada,  
 1026 *Quat. Sci. Review.*, 97, 148-169, 2014.  
 1027  
 1028 Meybeck, M.: Carbon, nitrogen, and phosphorus transport by world rivers, *Am. J. Sci.*, 282, 401-  
 1029 450, Available from: <http://earth.geology.yale.edu/~ajs/1982/04.1982.01.Maybeck.pdf>, 1982.  
 1030  
 1031 Milliman, J.D., and Syvitski J.P.M.: Geomorphic tectonic control of sediment discharge to the  
 1032 ocean: The importance of small mountainous rivers, *J. Geol.*, 100, 525-544, 1992.  
 1033  
 1034 Moore, R.D.: Introduction to salt dilution gauging for streamflow measurement part III: Slug  
 1035 injection using salt in solution, *Streamline Watershed Management Bulletin*, 8(2), 1-6, 2005.  
 1036  
 1037 Morrison, J., Foreman, M.G.G., and Masson, D.: A method for estimating monthly freshwater  
 1038 discharge affecting British Columbia coastal waters, *Atmosphere-Ocean*, 50, 1-8,  
 1039 doi:10.1080/07055900.2011.637667, 2012.

1040  
1041 Mulholland, P. and Watts, J.: Transport of organic carbon to the oceans by rivers of North  
1042 America: a synthesis of existing data, *Tellus*, 34, 176–186, doi:10.1111/j.2153-  
1043 3490.1982.tb01805.x, 1982.  
1044  
1045 Murphy, K., Stedmon, C., Graeber, D. and Bro, R.: Fluorescence spectroscopy and multi-way  
1046 techniques. *PARAFAC, Anal. Methods*, 5, 6557–6566, doi:10.1039/C3AY41160E, 2013.  
1047  
1048 Murphy K., Stedmon, C., Wenig, P., Bro, R.: OpenFluor- A spectral database of auto-  
1049 fluorescence by organic compounds in the environment, *Anal. Methods*, 6, 658-661,  
1050 DOI:10.1039/C3AY41935E, 2014.  
1051  
1052 Naiman, R.J.: Characteristics of sediment and organic carbon export from pristine boreal forest  
1053 watersheds, *Can. J. Fish. Aquat. Sci.*, 39(12), 1699-1718, doi:10.1139/f82-226, 1982.  
1054  
1055 Nakagawa, S., and Schielzeth, H.: A general and simple method for obtaining  $R^2$  from  
1056 generalized linear mixed-effects models, *Methods Ecol. Evol.*, 4(2): 133-  
1057 142. DOI: 10.1111/j.2041-210x.2012.00261.x, 2013.  
1058  
1059 Olefeldt, D., Roulet, N., Giesler, R. and Persson, A.: Total waterborne carbon export and DOC  
1060 composition from ten nested subarctic peatland catchments- importance of peatland cover,  
1061 groundwater influence, and inter-annual variability of precipitation patterns, *Hydrol. Process.*,  
1062 27, 2280-2294, doi:10.1002/hyp.9358, 2013.  
1063  
1064 Pinheiro, J., Bates, D., DebRoy, S., Sarkar, D., and R Core Team: *nlme: Linear and Nonlinear*  
1065 *Mixed Effects Models*, R package version 3.1-128, 2016.  
1066  
1067 Pojar, J., Klinka, K., and Demarchi, D.A.: Chapter 6, Coastal Western Hemlock Zone, in:  
1068 *Special Report Series 6, Ecosystems of British Columbia*, Meidiner, D., and Pojar, J. (Eds.),  
1069 Ministry of Forests, British Columbia, Victoria, 330 p., 1991.  
1070  
1071 Poulin, B., Ryan, J. and Aiken, G.: Effects of iron on optical properties of dissolved organic  
1072 matter, *Environ. Sci. Technol.*, 48, 10098–106, doi:10.1021/es502670r, 2014.  
1073  
1074 R Core Team, R: *A language and environment for statistical computing*, R Foundation for  
1075 *Statistical Computing*, Vienna, Austria, <http://www.R-project.org/>, 2013.  
1076  
1077 Raymond, P., Saiers, J. and Sobczak, W.: Hydrological and biogeochemical controls on  
1078 watershed dissolved organic matter transport: pulse-shunt concept, *Ecology*, 97, 5-16,  
1079 doi:10.1890/14-1684.1, 2016.  
1080  
1081 Regnier, P., Friedlingstein, P., Ciais, P., Mackenzie, F., Gruber, N., Janssens, I., Laruelle, G.,  
1082 Lauerwald, R., Luysaert, S., Andersson, A., Arndt, S., Arnosti, C., Borges, A., Dale, A.,  
1083 Gallego-Sala, A., Godd ris, Y., Goossens, N., Hartmann, J., Heinze, C., Ilyina, T., Joos, F.,  
1084 LaRowe, D., Leifeld, J., Meysman, F., Munhoven, G., Raymond, P., Spahni, R., Suntharalingam,

1085 P. and Thullner, M.: Anthropogenic perturbation of the carbon fluxes from land to ocean, *Nat.*  
1086 *Geosci.*, 6, 597–607, doi:10.1038/ngeo1830, 2013.

1087  
1088 Roddick, J.R.: *Geology, Rivers Inlet-Queens Sound, British Columbia, Open File 3278,*  
1089 *Geological Survey of Canada, Ottawa, Canada, 1996.*

1090  
1091 Royer, T.C., Coastal fresh water discharge in the northeast, Pacific, *J. Geophys. Res.*, 87, 2017-  
1092 2021, 1982.

1093  
1094 Runkel, R.L., Crawford, C.G., and Cohn, T.A.: Load Estimator (LOADEST): A FORTRAN  
1095 program for estimating constituent loads in streams and rivers, U.S. Geological Survey  
1096 Techniques and Methods Book 4, Chapter A5, 65 pp., 2004.

1097  
1098 Sanderman, J., Lohse, K.A., Baldock, J.A., and Amundson, R.: Linking soils and streams:  
1099 Sources and chemistry of dissolved organic matter in a small coastal watershed, *Water Resour.*  
1100 *Res.*, 45, W03418, doi:10.1029/2008WR006977, 2009.

1101  
1102 Spencer, R., Butler, K. and Aiken, G.: Dissolved organic carbon and chromophoric dissolved  
1103 organic matter properties of rivers in the USA, *J. Geophys. Res. Biogeosciences*, 117(G03001),  
1104 doi:10.1029/2011JG001928, 2012.

1105  
1106 Spencer, R.G., Hernes, P.J, Ruf, R., Baker, A., Dyda, R.Y., Stubbins, A., and Six, J.: Temporal  
1107 controls on dissolved organic matter and lignin biogeochemistry in a pristine tropical river,  
1108 Democratic Republic of Congo, *J. Geophys. Res.*, 115, G03013, doi:10.1029/2009JG001180,  
1109 2010.

1110  
1111 Stackpoole, S.M., Butman, D.E., Clow, D.W., Verdin, K.L., Gaglioti, B., and Striegl, R.: Carbon  
1112 burial, transport, and emission from inland aquatic ecosystems in Alaska, in: *Baseline and*  
1113 *projected future carbon storage and greenhouse-gas fluxes in ecosystems of Alaska*, Zhiliang, Z.,  
1114 and David, A. (Eds.), U.S. Geological Survey Professional Paper, 1826, 196 p., 2016.

1115  
1116 Stackpoole, S.M., Butman, D.E., Clow, D.W., Verdin, K.L., Gaglioti, B.V., Genet, H., and  
1117 Striegl, R.G.: Inland waters and their role in the carbon cycle of Alaska, *Ecol. Appl.*, Accepted  
1118 Author Manuscript, doi: 10.1002/eap.1552, 2017.

1119  
1120 Stedmon, C. and Bro, R.: Characterizing dissolved organic matter fluorescence with parallel  
1121 factor analysis: a tutorial, *Limnol. Oceanogr. Methods*, 6, 572–579,  
1122 doi:10.4319/lom.2008.6.572b, 2008.

1123  
1124 Stedmon, C. and Markager, S.: Tracing the production and degradation of autochthonous  
1125 fractions of dissolved organic matter by fluorescence analysis, *Limnol. Oceanogr.*, 50(5), 1415–  
1126 1426, doi:10.4319/lo.2005.50.5.1415, 2005.

1127  
1128 Stedmon, C., Markager, S., Bro, R., Stedmon, C., Markager, S. and Bro, R.: Tracing dissolved  
1129 organic matter in aquatic environments using a new approach to fluorescence spectroscopy, *Mar.*  
1130 *Chem.*, doi:10.1016/S0304-4203(03)00072-0, 2003.

1131  
1132 Stevenson, F.J.: *Humus Chemistry: Genesis, Composition, Reactions*, 2, Jon Wiley and Sons  
1133 Inc., New York, United States of America, 1994.  
1134  
1135 Symonds, M.R.E., and Moussalli, A.: A brief guide to model selection, multimodel inference,  
1136 and model averaging in behavioural ecology using Akaike's information criterion, *Behav. Ecol.*  
1137 *Sociobiol.*, 65:13-21, DOI: 10.1007/s00265-010-1037-6, 2011.  
1138  
1139 Tallis, H.: Kelp and rivers subsidize rocky intertidal communities in the Pacific Northwest  
1140 (USA), *Marine Ecology Progress Series*, 389, 8596, doi:10.3354/meps08138, 2009.  
1141  
1142 Tank, S., Raymond, P., Striegl, R., McClelland, J., Holmes, R., Fiske, G. and Peterson, B.: A  
1143 land-to-ocean perspective on the magnitude, source and implication of DIC flux from major  
1144 Arctic rivers to the Arctic Ocean, *Global Biogeochem. Cycles*, 26, GB4018,  
1145 doi:10.1029/2011GB004192, 2012.  
1146  
1147 Tank, S., Striegl, R.G., McClelland, J.W., and Kokelij, S.V.: Multi-decadal increases in  
1148 dissolved organic carbon and alkalinity flux from the Mackenzie drainage basin to the Arctic  
1149 Ocean, *Environ. Res. Lett.*, 11(5), doi:10.1088/1748-9326/11/5/054015, 2016.  
1150  
1151 Thompson, S.D., Nelson, T.A., Giesbrecht, I., Frazer, G., and Saunders, S.C.: Data-driven  
1152 regionalization of forested and non-forested ecosystems in coastal British Columbia with LiDAR  
1153 and RapidEye imagery, *Appl. Geogr.*, 69, 35–50, doi: 10.1016/j.apgeog.2016.02.002,  
1154 2016.  
1155  
1156 Trant, A.J., Nijland, W., Hoffman, K.M., Mathews, D.L., McLaren, D., Nelson, T.A.,  
1157 Starzomski, B.M.: Intertidal resource use over millennia enhances forest productivity, *Nature*  
1158 *Commun.*, 7, 12491, doi: 10.1038/ncomms12491, 2016.  
1159  
1160 van Hees, P., Jones, D., Finlay, R., Godbold, D. and Lundström, U.: The carbon we do not see-  
1161 the impact of low molecular weight compounds on carbon dynamics and respiration in forest  
1162 soils: a review, *Soil Biol. Biochem.*, 37, 1–13, doi:10.1016/j.soilbio.2004.06.010, 2005.  
1163  
1164 Wallin, M., Weyhenmeyer, G., Bastviken, D., Chmiel, H., Peter, S., Sobek, S. and Klemetsson,  
1165 L.: Temporal control on concentration, character, and export of dissolved organic carbon in two  
1166 hemiboreal headwater streams draining contrasting catchments, *J. Geophys. Res. Biogeosci.* 120,  
1167 832–846, doi:10.1002/2014jg002814, 2015.  
1168  
1169 Wang, T., Hamann, A., Spittlehouse, D.L., and Murdock, T.Q.: ClimateWNA- High resolution  
1170 spatial climate data for Western North America, *J. Appl. Meteorol. Climatol.*, 51, 16-29,  
1171 doi:dx.doi.org/10.1175/JAMC-D-11-043.1, 2012.  
1172  
1173 Weishaar, J.L., Aiken, G.R., Bergamaschi, B.A., Fram, M.S., Fujii, R. and Mopper, K.:  
1174 Evaluation of specific ultraviolet absorbance as an indicator of the chemical composition and

1175 reactivity of dissolved organic carbon, *Environ. Sci. Technol.*, 37, 4702–4708,  
1176 doi:10.1021/es030360x, 2003.

1177  
1178 Whitney, F.A., Crawford, W.R. and Harrison, P.J.: Physical processes that enhance nutrient  
1179 transport and primary productivity in the coastal and open ocean of the subarctic NE  
1180 Pacific, *Deep Sea Research Part II: Topical Studies in Oceanography*, 52, 681–706, 2005.

1181  
1182 Wickland, K., Neff, J., and Aiken, G.: Dissolved Organic Carbon in Alaskan Boreal Forest:  
1183 Sources, Chemical Characteristics, and Biodegradability, *Ecosystems*, 10, 1323-1340, 2007.

1184  
1185 Wilson, H.F. and Xenopoulos, M.A.: Effects of agricultural land use on the composition of  
1186 fluvial dissolved organic matter, *Nat. Geosci.*, 2, 37–41, doi:10.1038/ngeo391, 2009.

1187  
1188 Wolf, E.C., Mitchell, A.P., and Schoonmaker, P.K.: *The Rain Forests of Home: An Atlas of*  
1189 *People and Place*, Ecotrust, Pacific GIS, Inforain, and Conservation International, Portland,  
1190 Oregon, 24 pp., available at: [http://www.inforain.org/pdfs/ctrf\\_atlas\\_orig.pdf](http://www.inforain.org/pdfs/ctrf_atlas_orig.pdf), 1995.

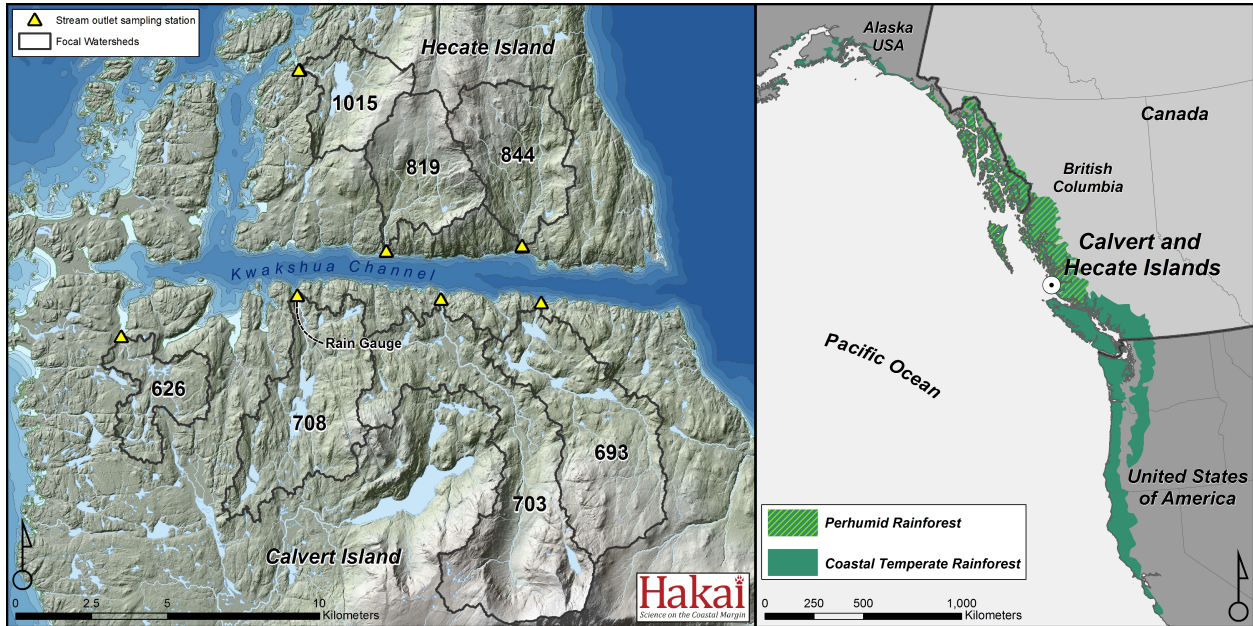
1191  
1192 Worrall, F., Burt, T., and Adamson, J.: Can climate change explain increases in DOC flux from  
1193 upland peat catchements?, *Sci. Total. Environ.*, 326, 95–112,  
1194 doi:10.1016/j.scitotenv.2003.11.022, 2004.

1195  
1196 Xenopoulos, M.A., Lodge, D.M., Frentress, J., Kreps, T.A., Bridgham, S.D., Grossman, E., and  
1197 Jackson, C.J.: Regional comparisons of watershed determinants of dissolved organic carbon in  
1198 temperate lakes from the Upper Great Lakes region and selected regions globally, *Limnol.*  
1199 *Oceanogr.*, 48(6), 2321-2334, 2003.

1200  
1201 Yamashita, Y. and Jaffé, R.: Characterizing the Interactions between Trace Metals and Dissolved  
1202 Organic Matter Using Excitation–Emission Matrix and Parallel Factor Analysis, *Environ. Sci.*  
1203 *Technol.*, 42, 7374–7379, doi:10.1021/es801357h, 2008.

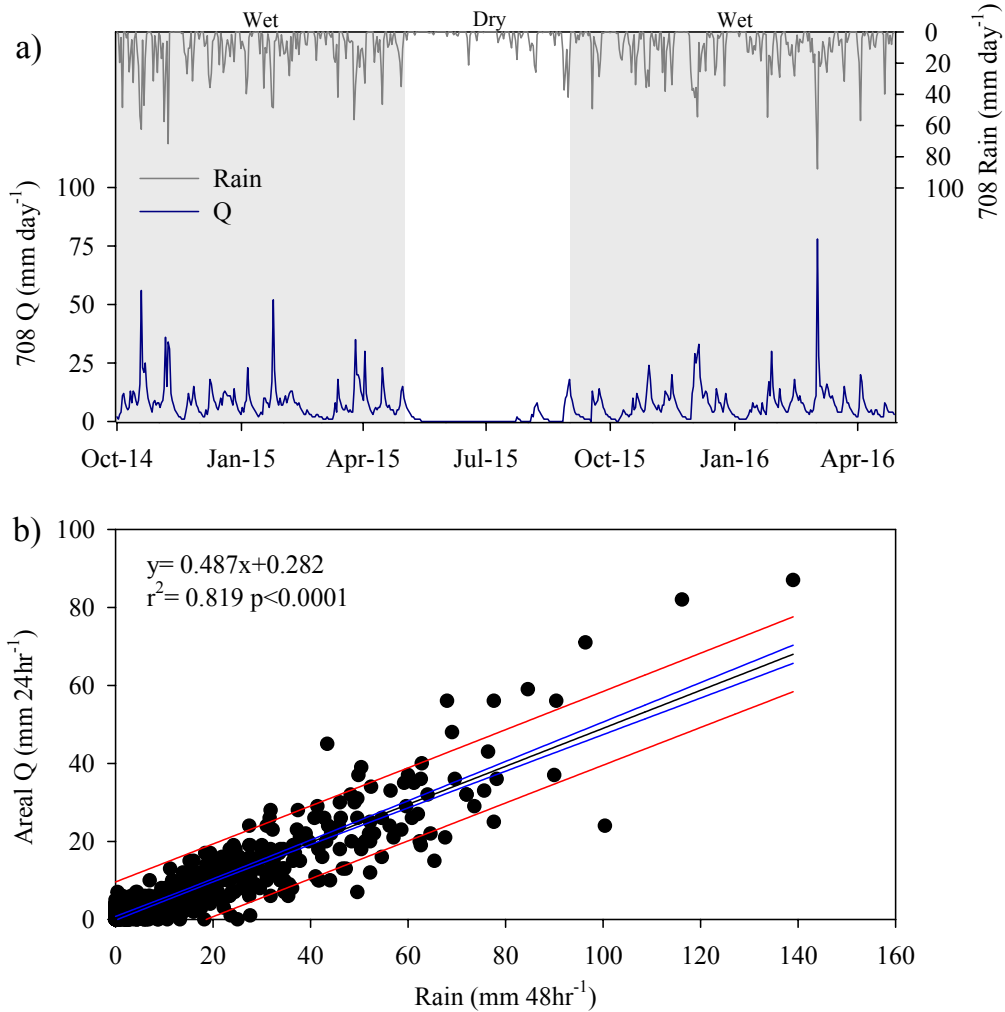
1204  
1205 Yamashita, Y., Kloepfel, B., Knoepp, J., Zausen, G. and Jaffé, R.: Effects of Watershed History  
1206 on Dissolved Organic Matter Characteristics in Headwater Streams, *Ecosystems*, 14, 1110–1122,  
1207 doi:10.1007/s10021-011-9469-z, 2011.

1208 **Figure 1.** The location of Calvert Island, British Columbia, Canada, within the perhumid region  
1209 of the coastal temperate rainforest (right) and the study area on Calvert and Hecate Islands,  
1210 including the seven study watersheds, corresponding stream outlet sampling stations, and  
1211 location of the rain gauge (left). Characteristics of individual watersheds are described in Table  
1212 1.  
1213



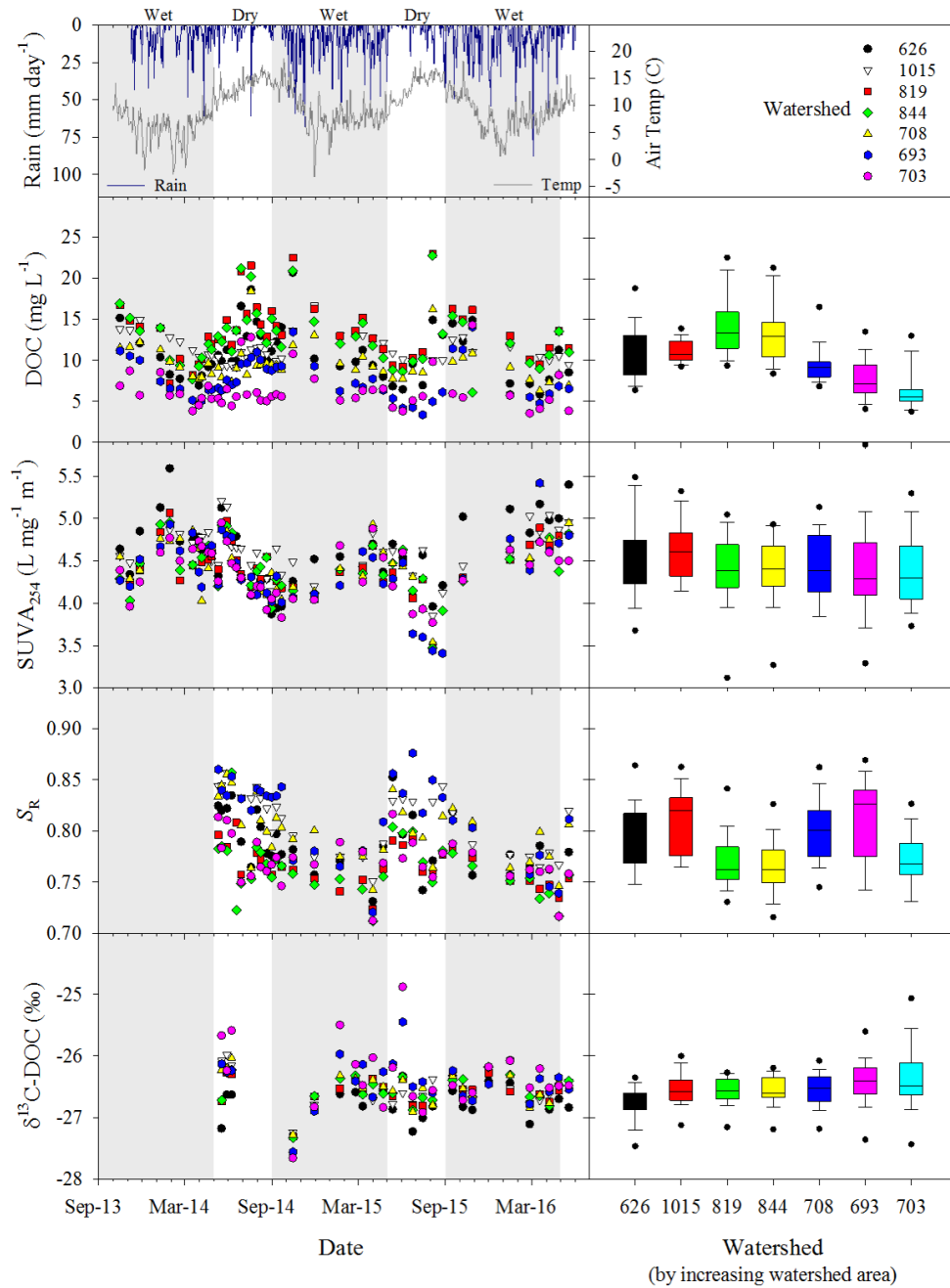
1214  
1215  
1216  
1217  
1218  
1219  
1220  
1221  
1222  
1223  
1224  
1225  
1226  
1227  
1228  
1229  
1230  
1231  
1232  
1233  
1234  
1235

1236 **Figure 2.** Hydrological patterns typical of watersheds located in the study area (a) the  
 1237 hydrograph and precipitation record from Watershed 708 for the study period of October 1,  
 1238 2015-April 30, 2016. Grey shading indicates the wet period (September 1-April 30) and the  
 1239 unshaded region indicates the dry period (May 1-August 30) (b) Correlation of daily (24 hour)  
 1240 areal runoff (discharge of all watersheds combined) to 48 hour total rainfall recorded at  
 1241 watershed 708. For the period of study, comparisons of daily runoff to 48-hr rainfall  
 1242 (runoff:rainfall mean= 0.92, std  $\pm$ 0.27) indicated rapid discharge response to rainfall.



1243  
 1244  
 1245  
 1246

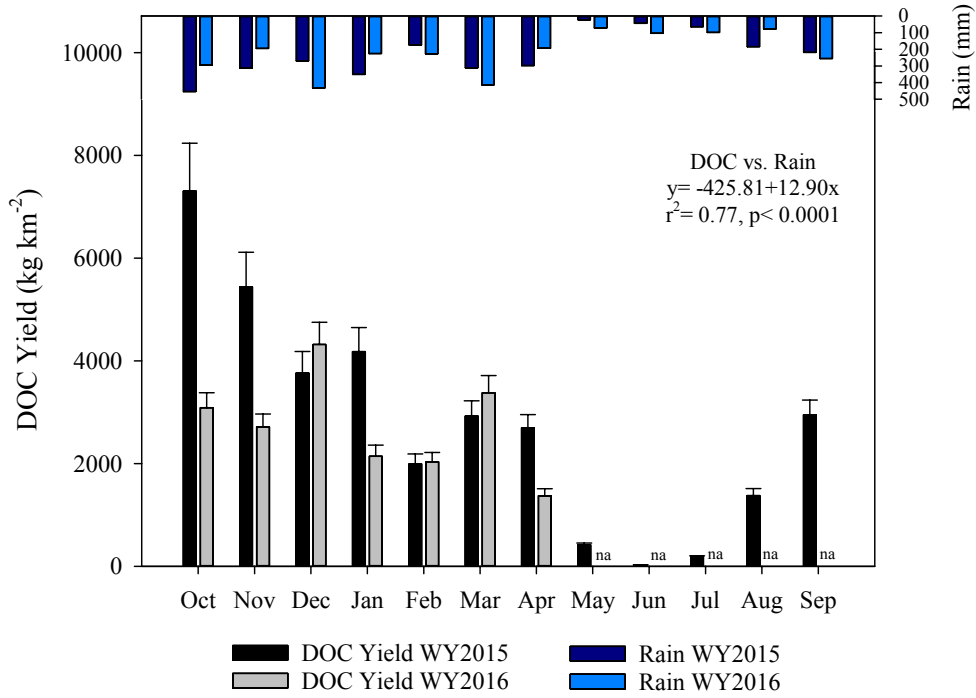
1247 **Figure 3.** Seasonal (timelines, by date) and spatial (boxplots, by watershed) patterns in DOC  
 1248 concentration and DOM composition for stream water collected at the outlets of the seven study  
 1249 watersheds on Calvert and Hecate Islands. Boxes represent the 25<sup>th</sup> and 75<sup>th</sup> percentile, while  
 1250 whiskers represent the 5<sup>th</sup> and 95<sup>th</sup> percentile. Daily precipitation and annual temperature are  
 1251 shown in the top left panel. Grey shading indicates the wet period (September 1-April 30) and  
 1252 the unshaded region indicates the dry period of each water year.  
 1253



1254

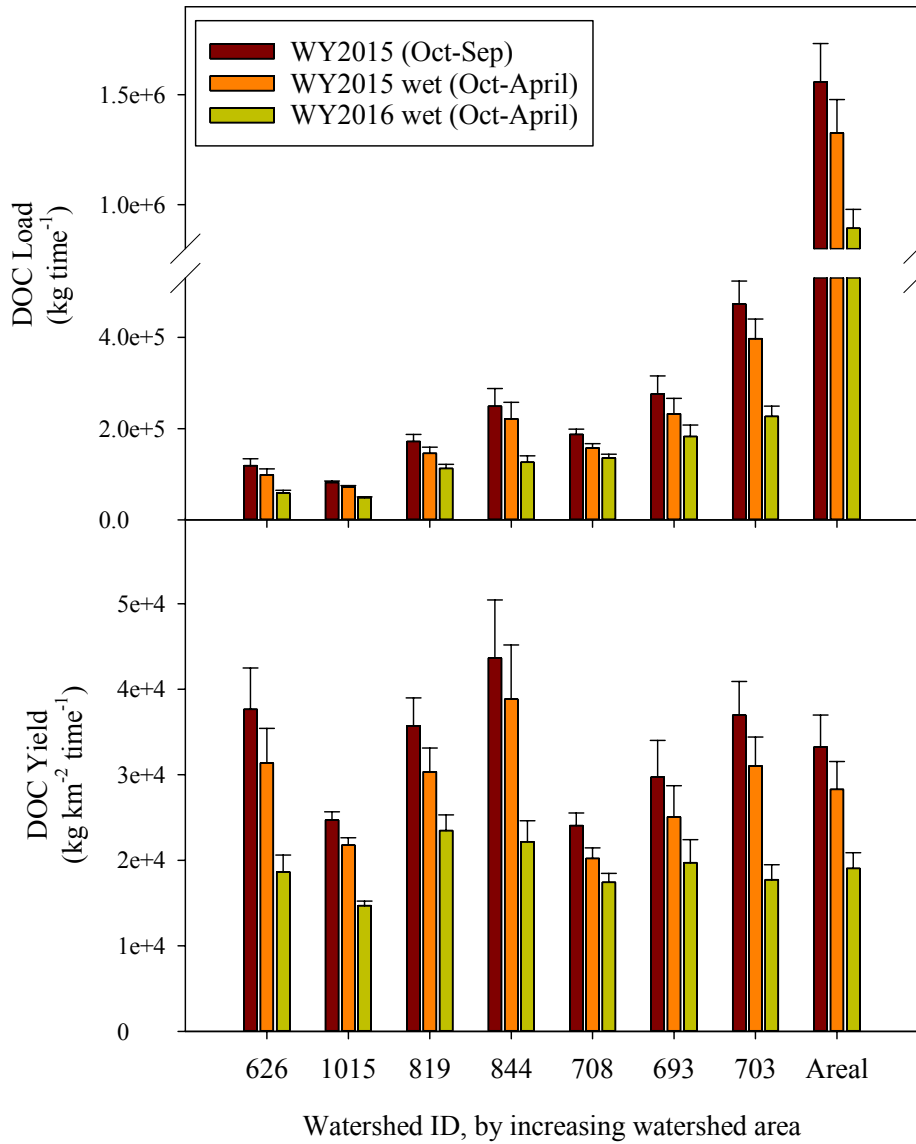


1255 **Figure 4.** Monthly areal DOC yields and precipitation for water year 2015 (WY2015) and the  
 1256 wet period (October 1-April 30) of water year 2016 (WY2016). Error bars represent standard  
 1257 error. Total rain and DOC yield were significantly correlated ( $r^2 = 0.77$ ) and months of higher  
 1258 rain produced higher DOC yields. In WY2015, the majority of DOC export (~94% of annual  
 1259 flux) occurred during the wet period (~88% of annual precipitation).



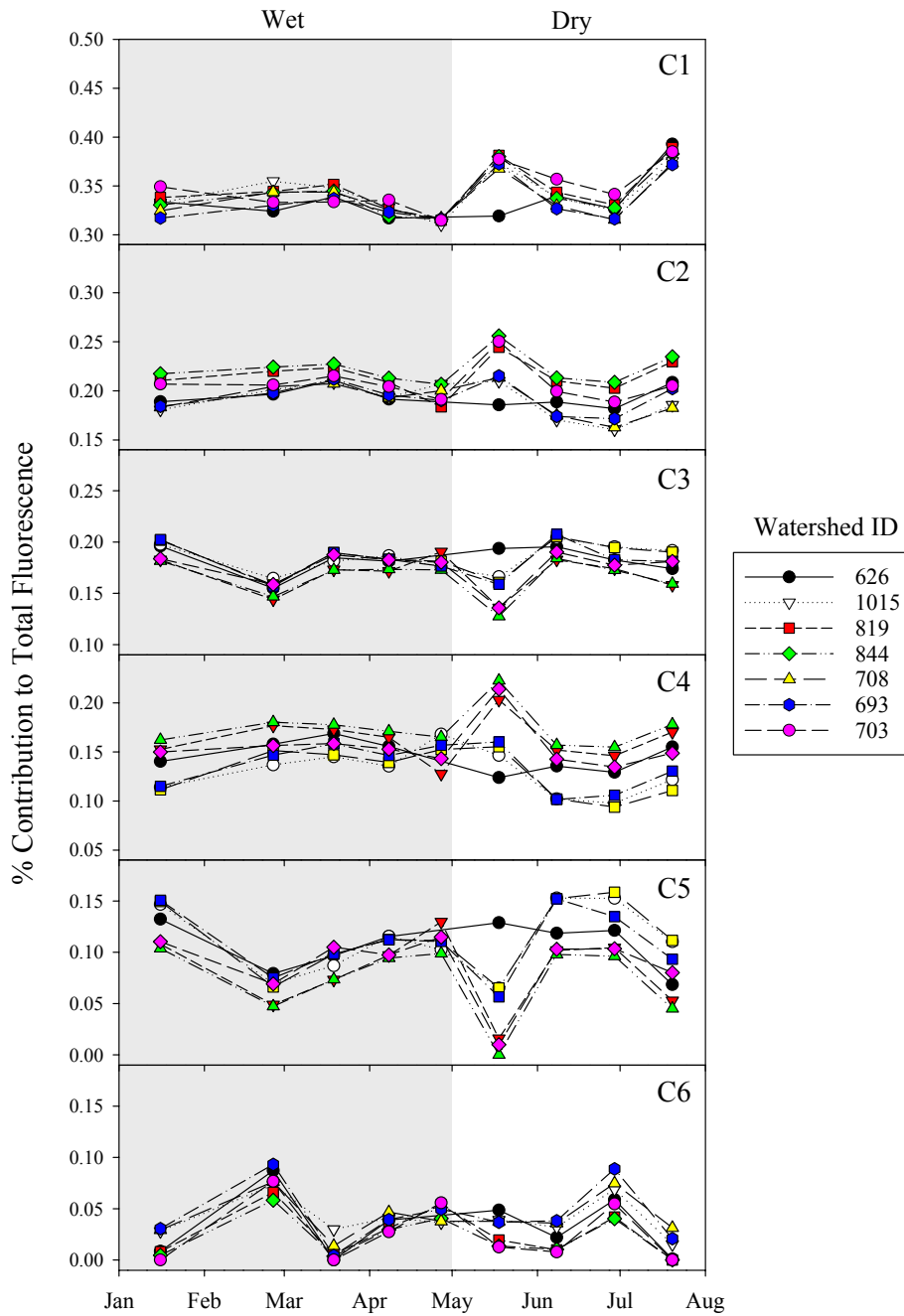
1260  
 1261  
 1262  
 1263  
 1264  
 1265  
 1266  
 1267  
 1268  
 1269  
 1270  
 1271  
 1272  
 1273  
 1274  
 1275  
 1276  
 1277

1278 **Figure 5:** DOC fluxes and yields for the seven study watersheds and the total area of study  
 1279 (“areal”, all watersheds combined) on Calvert and Hecate Islands for water year 2015 (WY2015;  
 1280 Oct 1 - Sep 30), and October 1- April 30 of the wet period for water year 2015 (WY2015 wet)  
 1281 and water year 2016 (WY2016 wet). Because DOC yields were only available for September in  
 1282 WY2015, this month was excluded from the wet period totals in order to make similar  
 1283 comparisons between years. Error bars represent standard error.



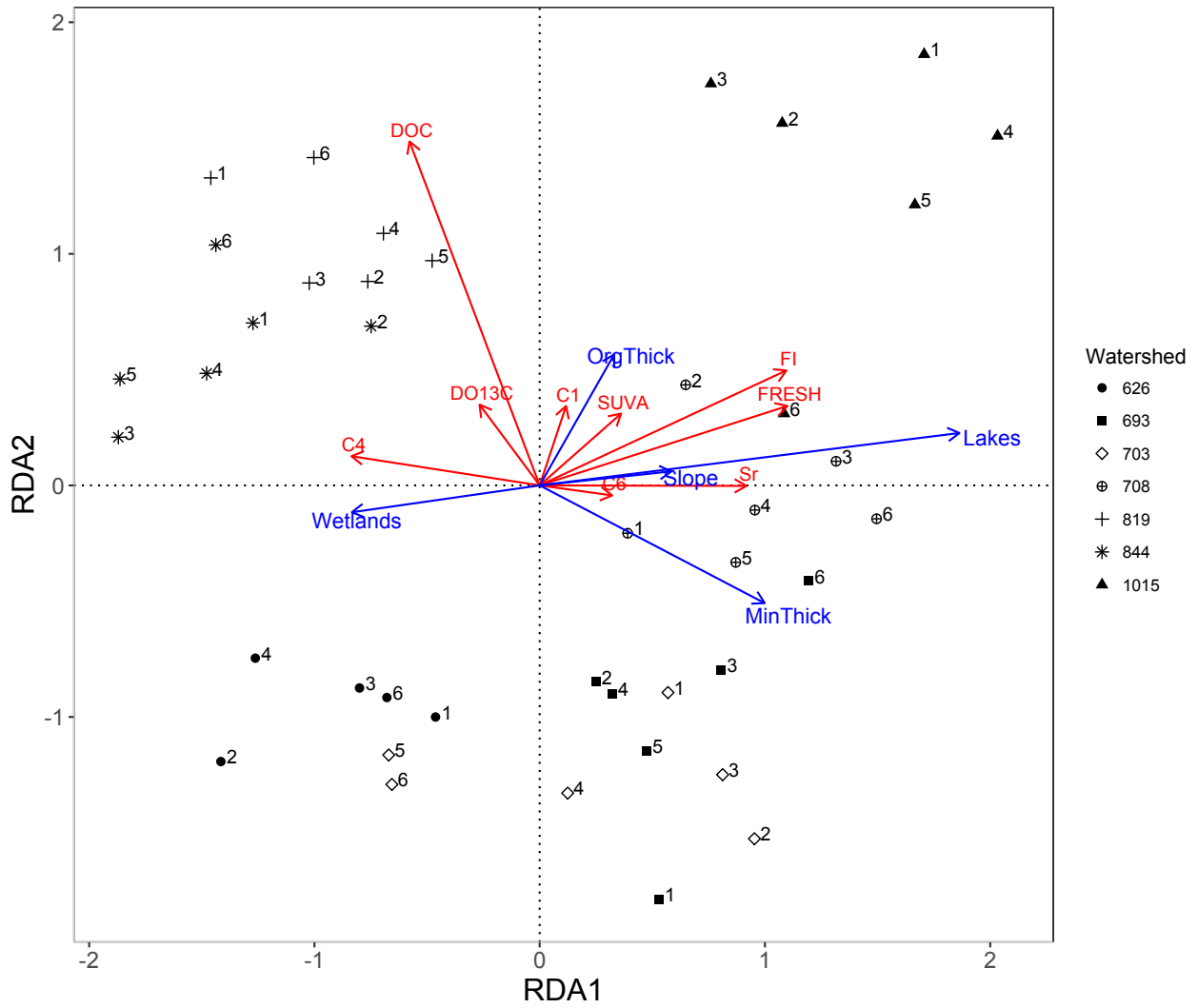
1284 **Figure 6:** Percent contribution of the six components identified in parallel factor analysis  
 1285 (PARAFAC) for samples collected every three weeks from January-July, 2016 from the seven  
 1286 study watersheds on Calvert and Hecate Islands. The grey shading indicates the wet period and  
 1287

1288 the unshaded region indicates the dry period. Note that while the y-axis for each panel has a  
 1289 range of 20%, the max and min for each y-axis varies by panel.



1290  
 1291 **Figure 7:** Results from the partial-Redundancy analysis (RDA; type 2 scaling) of DOC  
 1292 concentration and DOM composition versus watershed characteristics. Angles between vectors  
 1293 represent correlation, i.e., smaller angles indicate higher correlation. Symbols represent different

1294 watersheds, and numbers on symbols represent the sample month in 2016: 1= January, 2=  
 1295 February, 3= March, 4= early April, 5= late April, and 6= May.  
 1296



1297

1298 **Table 1:** Watershed characteristics, discharge, DOC concentrations, and DOC yields for the seven study watersheds on Calvert and  
 1299 Hecate Islands. Additional details on the methods used to determine watershed characteristics can be found in Supplemental Material.

Water- shed	Area (km <sup>2</sup> )	Avg. Slope (%)	Lakes (% Area)	Wetlands (% Area)	Avg. Depth Organic Soils (cm)	Avg. Depth Mineral Soils (cm)	Total Q Yield* (mm)	DOC* <sup>a</sup> (mg L <sup>-1</sup> )	Q- weighted Avg. DOC* (mg L <sup>-1</sup> )	DOC Annual Yield <sup>b</sup> WY2015* (Mg C km <sup>-2</sup> )	DOC Monthly Yield <sup>b</sup> Wet Season** (Mg C km <sup>-2</sup> )	DOC Monthly Yield <sup>b</sup> Dry Season*** (Mg C km <sup>-2</sup> )
626	3.2	21.7	4.7	48.0	39.4 ±24.3	30.8 ±8.3	3673	11.0 ±3.5	15.3	37.7 (31.9 – 44.2)	3.59 (3.05 – 4.18)	0.62 (0.49 – 0.77)
1015	3.3	34.2	9.1	23.8	39.5 ±17.2	33.7 ±8.6	3052	11.2 ±1.6	12.9	24.7 (23.6 – 25.8)	2.56 (2.45 – 2.78)	0.27 (0.25 – 0.28)
819	4.8	30.1	0.3	50.2	37.9 ±19.1	29.8 ±5.7	3066	14.0 ±3.5	19.3	35.7 (31.7 – 40.2)	3.80 (3.37 – 5.10)	0.57 (0.48 – 0.67)
844	5.7	32.5	0.3	35.2	35.4 ±18.0	29.1 ±6.4	4129	13.1 ±3.6	15.9	43.6 (34.2 – 54.9)	4.24 (3.36 – 5.30)	0.54 (0.36 – 0.77)
708	7.8	28.5	7.5	46.3	36.2 ±19.7	29.9 ±6.0	3805	9.5 ±2.4	10.9	24.1 (22.2 – 26.0)	2.67 (2.46 – 4.07)	0.38 (0.34 – 0.43)
693	9.3	30.2	4.4	42.8	35.4 ±16.1	30.2 ±6.4	5866	7.7 ±2.5	8.4	29.7 (25.9 – 34.0)	3.19 (2.79 – 4.94)	0.41 (0.32 – 0.52)
703	12.8	40.3	1.9	24.3	37.3 ±16.5	35.8 ±13.4	6058	6.3 ±2.6	9.0	37.0 (32.5 – 42.0)	3.48 (3.07 – 4.02)	0.64 (0.52 – 0.77)
All	46.9	32.7	3.7	37.1	37.4 ±17.7	32.2 ±9.2	4730	10.4 ±3.8	11.1	33.3 (28.9 – 38.1)	3.35 (2.94 – 4.40)	0.50 (0.41 – 0.62)

\* Calculated for water year 2015 (WY2015; Oct 1, 2014-Sep 30, 2015)  
 \*\* Wet period average monthly yield calculated from October-April and September, WY2015 and October-April, WY2016  
 \*\*\* Dry period average monthly yield calculated from May-August, WY2015  
<sup>a</sup> Mean ± standard deviation  
<sup>b</sup> Total ± 95% confidence interval

1301 **Table 2:** Spectral composition for the six fluorescence components identified using PARAFAC, including excitation (Ex.) and  
 1302 emission (Em.) peak values, percent composition across all samples, and likely structure and characteristics of the fluorescent  
 1303 component based on previous studies.

Component	Ex. (nm)	Em. (nm)	% Composition <sup>a</sup>	Potential structure/Characteristics	Previous studies with comparable results
C1	315	436	34.1 ±2.2 (31.1-39.3)	Humic-like, less processed terrestrial, high molecular weight, widespread but highest in wetland and forest environment	Garcia et al. 2015(C1); Graeber et al. 2012(C1); Walker et al. 2014(C1); Yamashita et al. 2011(C1); Cory & McKnight, 2005(C1)
C2	270/ 380	484	20.2 ±1.9 (16.1-25.6)	Humic-like, resembles fulvic acid, widespread, high molecular weight terrestrial	Stedmon and Markager, 2005(C2); Stedmon et al. 2003(C3); Cory & McKnight, 2005(C5)
C3	270	478	17.8 ±1.8 (12.8-20.8)	Humic-like, highly processed terrestrial; suggested as refractory	Stedmon & Markager, 2005(C1); Yamashita et al. 2010(C2)
C4	305/ 435	522	14.8 ±2.6 (9.4-22.3)	Not commonly reported, similarities to fulvic-like, contributed from soils	Lochmuller & Saavedra, 1986(E)
C5	325	442	9.8 ±3.5 (0.0-15.9)	Aquatic humic-like from terrestrial environments; autochthonous, microbial produced; may be photoproduced	Boehme & Coble, 2000(Peak C); Coble et al. 1998(Peak C); Stedmon et al., 2003(C3)
C6	285	338	3.4 ±2.5 (0.0-9.3)	Amino acid-like/Tryptophan-like. Freshly added from land, autochthonous. Rapidly photodegradable	Murphy et al. 2008(C7); Shutova et al. 2003(C4); Stedmon et al. 2007(C7); Yamashita et al. 2003(C5)

<sup>a</sup> Mean ± stdev (min-max) from all samples

1304